Seasonality and episodic variation in picoeukaryote diversity and structure reveal community resilience to disturbances in the North Pacific Subtropical Gyre

Yoshimi M. Rii,[1,2,†] Logan M. Peoples,[3,†] David M. Karl,[2,4] Matthew J. Church [ID][3*]
[1]Hawai'i Institute of Marine Biology, University of Hawai'i at Mānoa, Kāne'ohe, Hawai'i
[2]Center for Microbial Oceanography: Research and Education, University of Hawai'i at Mānoa, Honolulu, Hawai'i
[3]Flathead Lake Biological Station, University of Montana, Polson, Montana
[4]Department of Oceanography, University of Hawai'i at Mānoa, Honolulu, Hawai'i

Abstract

We examined variability in the euphotic zone (0–175 m) picoeukaryotic community based on time-series observations (2011–2013) at Station ALOHA in the North Pacific Subtropical Gyre. By sampling over scales ranging from daily to approximately monthly over 2.25 years, we evaluated the resilience of the picoeukaryotic community to seasonal- to episodic-scale physical disturbances, such as convective mixing and mesoscale processes, respectively. We quantified the frequency and intensity of disturbances that altered upper ocean light and nutrients in the context of the Hawaii Ocean Time-series program climatology, and evaluated picoeukaryotic community resilience based on shifts in dissimilarity in community structure at different depths in the euphotic zone. Our results suggest that in this stratified habitat, picoeukaryote communities are resilient on timescales of days to weeks in response to these physical disturbances, and that the juxtaposition of mesoscale and submesoscale disturbances on more predictable seasonality requires spatially and temporally resolved assessment of community response and resilience. We highlight the value of examining recent (days to weeks) physical forcing of the upper ocean for insight into the influences of physical habitat alterations that structure the contemporaneous plankton community.

The capacity of an ecosystem to sustain functionality (e.g., productivity, nutrient cycling) following disturbance is defined by the cumulative resilience of the biological community (Holling 1973; Walker et al. 2004). Resilience is quantified as the time required for a system to return to some predisturbed state, providing a quantifiable metric to assess ecosystem stability (Carpenter et al. 2001; Ives and Carpenter 2007). Thus, quantifying resilience requires time-resolved information, where the predisturbed reference state can be established (Rykiel 1985; Pickett et al. 1989). Resilience reflects the cumulative tolerance or flexibility of the biological community to disturbance, where the

bounds on resilience are shaped by the historical legacy of disturbance and solidified by natural selection.

Studying disturbance and resilience as forces shaping ecosystem stability in the open ocean is challenging, in part owing to a need for time-resolved observations to quantify the initial reference state of a system and due to the spatially heterogenous nature of the fluid environment (Stommel 1963; Karl and Church 2017). In the sunlit waters of the open ocean, plankton growth rates are rapid (generation times on the order of days or less), allowing fast physiological responses to temporal and spatial perturbations to the environment (Margalef 1978; Reynolds et al. 1993). Such rapid response times suggest that studying time-varying changes in plankton population structure could prove to be a powerful tool for quantifying the resilience of aquatic systems (Reynolds et al. 1993; Shade et al. 2012). This may be particularly true for subtropical ocean gyres where relative constancy of environmental conditions, together with expansive species diversity, appear to promote ecosystem stability (Hayward and McGowan 1979; Venrick 1993). However, planktonic communities in subtropical gyres may be particularly susceptible to disturbances whose frequencies or intensities fall outside the normal envelope of variability.

Open ocean disturbances come in many forms and across a continuum of time and space scales. Pulsed, event-scale

disturbances, such as storms, eddies, and submesoscale filaments physically modify the upper ocean at spatial scales ranging from a few to hundreds of kilometers, driving subsequent biological responses over timescales ranging from days to weeks (DiTullio and Laws 1991; McGillicuddy et al. 1998; Cullen et al. 2002). Short duration, high frequency events, such as submesoscale features and internal waves, can alter depth distributions of plankton and nutrients relative to the upper ocean light gradient (Karl et al. 2003). Similarly, mesoscale eddies alter the vertical position of the pycnocline, resulting in local-scale disruption to rates of plankton growth and community structure and ultimately modifying ecosystem function (McGillicuddy et al. 1998; Letelier et al. 2000; Barone et al. 2019). Episodic events are superimposed on seasonally recurring physical dynamics, such as stratification and turbulent mixing, which alter light availability and nutrient supply, with subsequent recurrent changes in plankton biomass, community structure, net productivity, and export (Sverdrup 1953; Venrick 1993; Karl et al. 2003). Lower frequency disturbances (e.g., sub-decadal to decadal scales), such as those controlled by basin-scale ocean-climate oscillations (e.g., El-Niño Southern Oscillation, ENSO), have also been shown to modify oceanic plankton community structure in the open sea (Karl et al. 1995; Corno et al. 2007; Bidigare et al. 2009). In some cases, infrequent, but intense, "pulsed" disturbances, as well as continuous, low-frequency "pressed" disturbances can be so disruptive that they push the system to a new regime or alternate state (Folke et al. 2004).

Emergent biological responses to disturbances can be complex, deriving from feedbacks among multiple interacting components of the ecosystem, with the resulting responses often nonlinear (Sugihara and May 1990). For example, in large regions of the ocean, predicted climate-driven increases in stratification have the potential to reduce turbulent nutrient exchange (Sarmiento et al. 1998; Polovina et al. 2008), stimulating chaotic oscillations in phytoplankton biomass and community structure (Huisman et al. 2006). Developing robust statistical tools to better understand the mechanisms and identify specific feedbacks underlying such complexity requires time-resolved observations conducted across scales ranging from those matching plankton generation times (daily) to those capturing seasonal- to decadal-scales of climate variability.

The North Pacific Subtropical Gyre (NPSG) is one of the largest biomes on Earth (Karl 1999). The upper ocean of the NPSG has historically been considered a physically and biologically stable system (Hayward and McGowan 1979; Venrick 1999), owing in large part to the latitudinal position of the gyre, with low seasonality in solar energy input and basin-scale spatial homogeneity in physical and biological structure. The perennial source of light energy available in this ecosystem fuels rapid phytoplankton growth and establishes a thermally stratified upper ocean (Karl and Lukas 1996). Together, these dynamics impose a two-layer upper ocean habitat, where the light-saturated upper euphotic zone is persistently devoid of bioavailable nutrients, while the dimly lit lower euphotic zone remains relatively enriched in nutrients. Plankton communities, including phytoplankton (Venrick 1993; Li et al. 2013) and heterotrophic protists (Hu et al. 2018; Ollison et al. 2021), demonstrate discrete vertical partitioning across this upper ocean light-nutrient gradient. Recycling of nutrients through tightly coupled food web dynamics drives the majority of biomass production in the well-lit upper ocean (Karl and Church 2017), resulting in low fluctuations in plankton biomass and export. The two layers of the upper ocean habitat experience physical disruption at different frequencies and intensities, with the well-lit region undergoing strong seasonal modification, while the dimly lit region experiences frequent perturbation arising from submesoscale- to mesoscale-driven vertical fluctuations in the pycnocline (Church et al. 2009; Johnson et al. 2010; Barone et al. 2019).

The oligotrophic conditions of the NPSG waters favor proliferation of picoplankton (≤ 3 μm diameter; Karl 1999, Rii et al. 2016). Due in large part to the >30 years of time-resolved, Eulerian (fixed in space) observations conducted at Station ALOHA by the Hawaii Ocean Time-series (HOT) program, much is known about the variability in abundances, productivity, and composition of phytoplankton in this ecosystem (e.g., Campbell and Vaulot 1993; Letelier et al. 1993; Venrick 1997). Expanded use of genomic techniques has provided additional insights into temporal and vertical variation in diversity and metabolic functioning of bacteria and archaea (DeLong et al. 2006; Bryant et al. 2016; Mende et al. 2017); less is known about variability of the eukaryotic plankton in the NPSG. Single-celled protists account for the majority of eukaryotic diversity (de Vargas et al. 2015; Caron et al. 2017; Keeling and Burki 2019) and these organisms have been the focus of several recent studies in the NPSG (Hu et al. 2018; Ollison et al. 2021). These eukaryotic plankton are sensitive to perturbations in light and nutrients (Alexander et al. 2015), with important subsequent biogeochemical impacts (Mahaffey et al. 2012; Rii et al. 2018). Furthermore, improved understanding of their responses to such perturbations, in metabolic rates and population structure with respect to their functional diversity, metabolic processes, and species interactions (Caron et al. 2017), is important for elucidating biogeochemical dynamics and community resilience. To date, the resilience of the picoplankton community, specifically the responsiveness of the abundant picoeukaryotes to seasonal and episodic disturbances, remains largely unexplored.

In this study, we examined temporal variability in the euphotic zone (0–175 m) picoeukaryote community based on Eulerian time series observations (2011–2013) at Station ALOHA. By sampling a spatially fixed point over timescales ranging from daily to approximately monthly over 2.25 years, we quantified the frequency and intensity of disturbances in both the upper and lower regions of the euphotic zone. Through these analyses, we evaluated the resilience of the picoeukaryote community in response to seasonal and episodic physical disturbances.

Methods

Shipboard sampling and measurements of seawater biogeochemistry

Samples were collected from eight discrete depths (5, 25, 45, 75, 100, 125, 150, and 175 m) on 19 research cruises to Station ALOHA (22.75°N, 158°W) in the NPSG between February 2011 and May 2013. All sampling occurred within a ~10-km radius circle centered at Station ALOHA, defining a surface area encompassing ~314 km². This included 18 approximately monthly, 4-day HOT program cruises (between H230 to H252) and 1 cruise (HOE-DYLAN 5; HD5) where samples were collected at approximately weekly timescales (1). This latter cruise was part of a more intensive shipboard sampling campaign in 2012 (Wilson et al. 2015). Seawater from discrete depths was collected in 12-L polyvinylchloride bottles affixed to a 24-bottle rosette sampler, equipped with a Sea-Bird 911 + conductivity, temperature, and pressure sensor package. Seawater for subsequent analyses of nutrient concentrations, picoplankton cell counts, and cellular DNA were collected once each on different days during the 4-day HOT cruise. More intensive sampling was performed on two cruises: DNA profiles were collected once each on 10 July 2012, 16 July 2012, and 22 July 2012 (during HD5) to examine weekly scale variability, and once each on 06 March 2013 and 07 March 2013 (during H250) to examine daily variability in picoeukaryote communities.

Daily vertical profiles of midday downwelling photosynthetically active radiation (PAR; 400–700 nm) and incident PAR were measured using a HyperPro radiometer, and a LICOR LI-1500 logger with a cosine collector, respectively. Daily PAR (mol quanta m^{-2} d^{-1}) at discrete depths was calculated based on measured attenuation coefficients (K_{PAR}) together with daily-integrated incident PAR measurements. The mixed layer depth was defined as the depth where a 0.125 kg m^{-3} potential density offset was observed relative to the surface ocean (Brainerd and Gregg 1995). Determinations of nitrate + nitrite (N+N) and phosphate (PO_4^{3-}) concentrations in the upper 100 m relied on high-sensitivity chemiluminescent methods (Garside 1982; Dore and Karl 1996) and the MAGnesium-Induced Co-precipitation method (MAGIC; Karl and Tien 1992), respectively. Concentrations of N + N, PO_4^{3-}, and silicic acid ($Si[OH]_4$) at depths >100 m were measured colorimetrically using a three-channel Bran + Luebbe Autoanalyzer III. Photosynthetic picoeukaryote cell abundances were distinguished and quantified using a Cytopeia Influx Mariner™ flow cytometer based on forward scatter and fluorescence characteristics. Concentrations of total chlorophyll *a* (TChl *a* = monovinyl chlorophyll *a* + divinyl chlorophyll *a*) were obtained from filter extracts detected using high-performance liquid chromatography following protocols described in Bidigare et al. (2005). All HOT program data used in this study are available at http://hahana.soest.hawaii.edu/hot/hot-dogs/interface.

High-frequency physical habitat measurements

High-frequency temperature and salinity measurements were obtained from an instrumented physical and meterological bottom-moored buoy termed the Woods Hole Oceanographic Institution Hawaii Ocean Time-series Station (WHOTS), which is deployed on the edge of the Station ALOHA circle. This mooring is equipped with subsurface Sea-Bird SeaCAT sensors (collecting data at < 10 min sampling intervals). For this study, we used selected data deriving from WHOTS 7, 8, and 9 deployments (spanning July 2010 through July 2014, http://www.soest.hawaii.edu/whots/). Measurements of daily sea-level anomaly (SLA) were downloaded in October 2019 from Copernicus (http://marine.copernicus.eu/faq/ssaltoduacs-integrated-sealevel-anomalies-products-changes-updates/?idpage=169/#FtpAccess), and seasonality and the long-term linear increase associated with SLA observations in this region were removed to obtain SLA$_{corr}$ (Barone et al. 2019; Karl et al. 2021).

We defined disturbances based on examining physical processes that resulted in perturbations to upper ocean light and nutrient gradients. Disturbances stemming from convective mixing were defined as those occasions where the mixed layer depth was deeper than the depth of the 1% surface PAR isopleth. We further defined disturbances based on mesoscale physical processes as those occasions when SLA$_{corr}$ ≥ 5 cm or ≤ −5 cm, corresponding approximately to the highest and lowest quartile measured throughout 1993–2015 HOT climatological measurements of SLA$_{corr}$ (Barone et al. 2019). With this qualification and based on the frequency of our shipboard sampling, we only consider mesoscale events as disturbances in these analyses, and do not consider submesoscale filaments, inertial oscillations, and internal waves whose influence on the pycnocline would not be captured by variations in SLA$_{corr}$.

Nucleic acid sample collection, extraction, and quantification

Seawater samples (2 L) for subsequent extraction of planktonic DNA were collected into acid-washed polyethylene bottles and sequentially filtered using a peristaltic pump onto 25 mm diameter, 3 μm pore size polycarbonate membranes (Millipore Isopore™), followed by filtration through 25 mm diameter, 0.2 μm pore size polyethersulfone filters (Pall Supor®). After filtration, filters were placed in sterile 1.5 mL microcentrifuge tubes, immediately flash-frozen in liquid nitrogen, and stored at −80°C until analyzed. Back in the shore-based laboratory, DNA from the 0.2 μm filter membranes was extracted and purified using the QIAGEN DNeasy Plant Mini Kit including a bead-beating step (with 0.1 and 0.5 mm beads) and Proteinase K (QIAGEN) for additional cell disruption and lysing (Rii et al. 2018). Extracts were eluted in 200 μL of nuclease-free PCR grade water and quantified fluorometrically (Qubit dsDNA high sensitivity assay kit; Thermo-Fisher Scientific).

Table 1. Dates of sampling, and physical and biogeochemical parameters during this study.

Cruise	Dates of cruise	Season*	SLA_{corr} (cm)†	Mixed layer depth (m)‡	Surface PAR (mol quanta m^{-2} d^{-1})	0–75 m N+N§ (mmol N m^{-2})	100–175 m N+N§ (mmol N m^{-2})	0–75 m PPE§ ($\times 10^{11}$ cells m^{-2})	100–175 m PPE§ ($\times 10^{11}$ cells m^{-2})
H230	27 Feb 2011–03 Mar 2011	Winter	−1.4 (−1.7/1.1)	40 (16–64)	34.5	0.23	93.2	0.75	0.90
H233‖	18–22 Jul 2011	Summer	7.7 (7.1/8.2)	78 (65–94)	44.1	0.26	25.5	0.78	0.84
H234¶	29 Aug 2011–01 Sep 2011	Summer	−5.4 (−5.6/−5.1)	48 (33–65)	41.7	0.17	76.3	0.46	0.46
H235	25–28 Sep 2011	Fall	−3.8 (−3.9/−3.6)	35 (19–55)	36.3	0.18	52.0	0.53	0.68
H236¶	03–11 Nov 2011	Fall	−8.0 (−8.7/−7.3)	57 (38–68)	n/a	0.13	88.8	0.97	0.63
H239#	17–21 Jan 2012	Winter	−1.5 (−1.6/−1.4)	98 (39–142)	28.7	0.17	45.6	0.73	0.44
H240	23–27 Mar 2012	Spring	−4.3 (−4.5/−3.9)	64 (42–85)	n/a	0.32	24.7	n/a	n/a
H241‖	30 Apr 2012–04 May 2012	Spring	6.0 (5.8/6.3)	114 (104–135)	44	0.16	11.5	0.74	0.69
H242	29 May 2012–02 Jun 2012	Spring	0.2 (−0.1/0.5)	36 (29–46)	48.4	0.24	22.0	0.72	0.96
H243	25–29 Jun 2012	Summer	0.9 (0.3/1.4)	73 (61–85)	42.8	0.49	51.8	0.85	0.81
HD5¶	08–28 Jul 2012	Summer	−5.0 (−6.0/−3.8)	58 (16–83)	43.25	0.23	49.7	0.82	0.73
H245	16–20 Aug 2012	Summer	1.5 (1.4/1.5)	34 (25–42)	n/a	0.56	21.9	0.82	0.66
H246	13–17 Sep 2012	Fall	3.2 (2.8/3.6)	59 (44–71)	41.7	0.27	14.9	0.72	0.70
H247	06–10 Oct 2012	Fall	3.0 (2.9/3.1)	60 (40–73)	35.8	0.25	14.3	0.47	0.49
H248‖	02–06 Dec 2012	Winter	6.3 (6.2/6.3)	92 (71–113)	15.2	0.29	70.7	0.50	0.54
H249‖,#	11–15 Feb 2013	Winter	5.6 (4.8/6.4)	111 (46–164)	24.1	0.32	17.5	1.24	1.00
H250‖,#	05–09 Mar 2013	Spring	6.5 (5.5/7.4)	126 (16–165)	39	0.32	30.9	1.31	0.79
H251	04–08 Apr 2013	Spring	−2.5 (−3.5/−1.5)	77 (34–132)	38.2	0.35	16.8	1.08	0.85
H252‖	16–20 May 2013	Spring	7.2 (6.9/7.3)	39 (15–52)	n/a	0.32	10.2	1.15	0.74

n/a, data not available.
*Seasonal designations were based on the first day of the cruise: Winter (December, January, February); Spring (March, April, May); Summer (June, July, August); Fall (September, October, November).
†Mean (min/max) of SLA_{corr} during the specified cruise.
‡Mean (range) of mixed layer depth calculated from all CTD casts conducted during the specified cruise.
§Depth-integrated N+N and photosynthetic picoeukaryote (PPE) cell abundances.
‖Episodic mesoscale disturbance event as defined by occurrences when cruise-averaged $SLA_{corr} \geq 5.0$ cm.
¶Episodic mesoscale disturbance event as defined by occurrences when cruise-averaged $SLA_{corr} \leq -5.0$ cm.
#Seasonal mixing disturbance event as defined by when the mixed layer depth deepened to below 1% surface PAR isopleth.

PCR amplification and sequence analyses

The hypervariable V9 region of 18S rRNA genes was amplified (in triplicate reactions per sample) using PCR primers 1391F (5′-GTACACACCGCCCGTC-3′; *Saccharomyces cerevisiae* NCBI GenBank Accession #U53879 position 1629–1644) and Euk Br (5′-TGATCCTTCTGCAGGTTCACCTAC-3′; *S. cerevisiae* NCBI GenBank Accession #U53879 position 1774-1797) following the methods outlined in Amaral-Zettler et al. (2009). Triplicate PCR products were pooled, fragment size was determined visually by gel electrophoresis, and DNA concentrations were subsequently quantified fluorometrically (Thermo-Fisher Scientific). From each sample, ~50 ng of PCR product was combined and purified and the quality of the resulting pooled PCR products was determined on a Bioanalyzer 2100 (Agilent). Paired-end sequencing (300 cycles) was conducted using an Illumina MiSeq at the University of Hawai'i Core Functional Genomics Facility.

Sequences were merged using PEAR and quality-filtered with reads trimmed to 100–150 bp, a maximum expected error of 1%, no ambiguous bases allowed, and an average Phred quality threshold > 34. Reference-based and de novo chimeras were detected and removed using USEARCH v7.0.1090 using the SILVA 119 database pre-clustered at 97% sequence identity (Quast et al. 2013). Remaining reads were clustered using UCLUST v1.2.22q (max accepts = 20, max rejects = 500) into operational taxonomic units (OTUs) using subsampled open-reference OTU picking through the QIIME pipeline (Caporaso et al. 2010). OTUs were first clustered with the SILVA 119 database and then clustered de novo at the 97% 18S rRNA gene identity thresholds. The centroid sequence within each OTU was selected as the representative sequence, and sequences that failed to align using PyNAST (minimum percent identification 0.75) were removed. Singletons (OTUs composed of only one sequence in the data set) and OTUs present in only one sample were removed. Taxonomy was assigned to representative sequences with BLAST (max E value/expectation threshold at 1e-30) using a preclustered PR^2 database v.4.12.0 (Guillou et al. 2013). A total of 29,062 distinct picoeukaryote OTUs at 97% sequence similarity from an average sequencing depth of ~29,000 sequences per sample were retrieved after removal of metazoan and bacterial OTUs, with 18% of OTUs not able to be classified at any taxonomic level. After rarefaction to equal sequencing depth, each sample contained 9100 sequences for a total of 21,040 OTUs. Raw sequence data was deposited into NCBI's Sequence Read Archive as BioProject ID PRJNA351881 (accession SRP092782).

Statistical analyses

Sequencing reads were processed with the package phyloseq (McMurdie and Holmes 2013) and vegan (Oksanen et al. 2013) within R 3.6.1. Samples were rarefied to even sampling depth, and alpha diversity analyses were performed using the Chao1 and Shannon indices to identify differences between depths. Differentially abundant taxa between depths were identified using the package DeSEQ2 by grouping samples within either the upper (5–75 m) or lower (100–175 m) euphotic zone. DeSEQ2 comparisons were performed on samples without rarefaction; however, minimum sequence abundance thresholds of 0.1% of the dataset at the OTU level were used to remove low abundance lineages. Graphical outputs were constructed with Ocean Data View 4.6.2 and with the package ggplot2 (Wickham 2009) in R. When possible, we determined resilience by evaluating the timescales over which communities responded to disturbance and returned to pre-disturbance conditions; community response was measured by beta-diversity comparisons between samples using the Bray–Curtis dissimilarity index. Dissimilarities were visualized in both a pairwise manner, in relation to a single sample or depth, and via multiple sample comparisons using nonmetric multidimensional scaling (NMDS) ordinations. Permutational ANOVA (PERMANOVA) with the function adonis was used to determine if environmental parameters significantly explained community composition.

Results

Two-layer euphotic zone habitat

During our study, physical, biological, and chemical features of the euphotic zone (0–175 m) were consistent with HOT program climatology, including a persistently low-nutrient, high-light habitat (< 75 m), a deeper, relatively nutrient-enriched low-light region (100–175 m), and seasonally variable stratification, with shallow mixed layers during the summer and fall and deeper mixed layers in the winter and spring (Table 1, Figs. 1, 2a,b, Supporting Information Fig. S1b). SLA_{corr} ranged between approximately − 8.0 and 7.7 cm, with most observations falling within the 5 and 95 percentiles of SLA_{corr} variations at Station ALOHA (Barone et al. 2019; Table 1, Fig. 2c,d, Supporting Information Fig. S1a). Anomalously deep mixed layer depths often coincided with periods of positive SLA_{corr} in our dataset, and more generally in the HOT program observations (Table 1, Supporting Information Fig. S1c). In the lower regions of the euphotic zone (e.g., at 125 m), PAR ranged from 0.2 to 0.8 mol quanta m^{-2} d^{-1} in spring and summer, decreasing to between 0.02 and 0.2 mol quanta m^{-2} d^{-1} in fall and winter (Table 1). Notably, nutrient concentrations tended to co-vary with vertical oscillations in isopycnal surfaces (Fig. 1b); consistent with previous analyses (Barone et al. 2019), elevated PO_4^{3-} concentrations in the upper 75 m often coincided with periods when SLA_{corr} was positive (Supporting Information Fig. S2a), although this pattern was less apparent when SLA_{corr} exceeded 5 cm. In contrast, N+N concentrations were inversely related to SLA_{corr} in the lower euphotic zone (Table 1, Supporting Information Fig. S2b). A deep chlorophyll maximum layer (DCML) was evident between 100 and 150 m (Fig. 1c), and depth-integrated cell inventories of
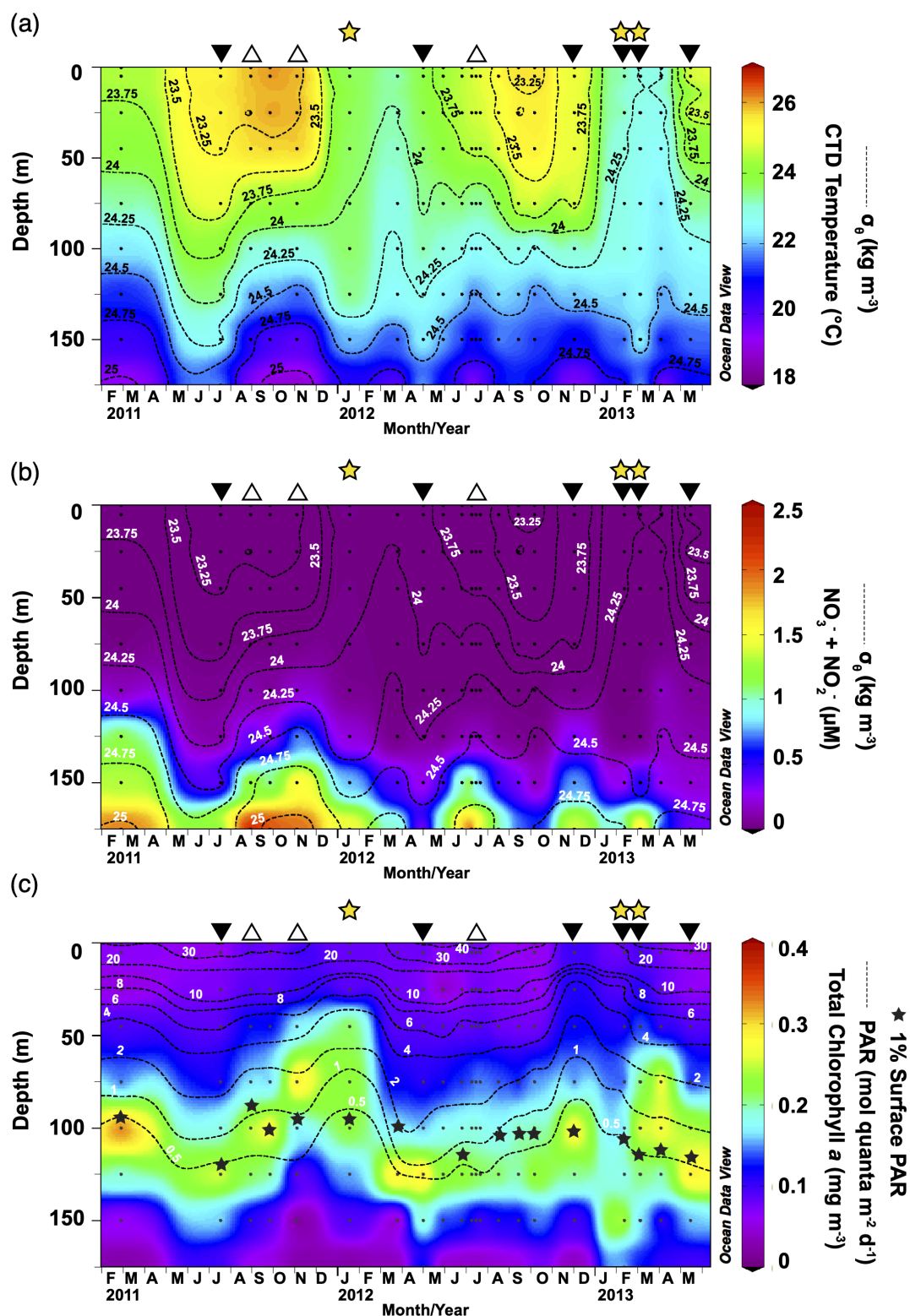
Fig. 1. Temperature and nutrients are vertically structured at Station ALOHA, with a persistent DCML. Contour plots depicting upper ocean (0–175 m) biogeochemistry: Temporal and vertical variations in **(a)** seawater temperature, **(b)** N+N concentrations, and **(c)** TChl *a* concentrations between February 2011 and May 2013. Superimposed contour lines (dashed) indicate (a and b) isopycnal density surfaces (σ_θ) and (c) PAR isolumes. Black circles indicate discrete depths where samples for picoeukaryote community structure was examined, and black stars indicate depths of the 1% surface PAR isopleth. Seasonal mixing events (yellow stars), and episodic mesoscale events when cruise-averaged $SLA_{corr} \leq -5.0$ cm (open triangles) and $SLA_{corr} \geq 5.0$ cm (black triangles) are marked above each panel.
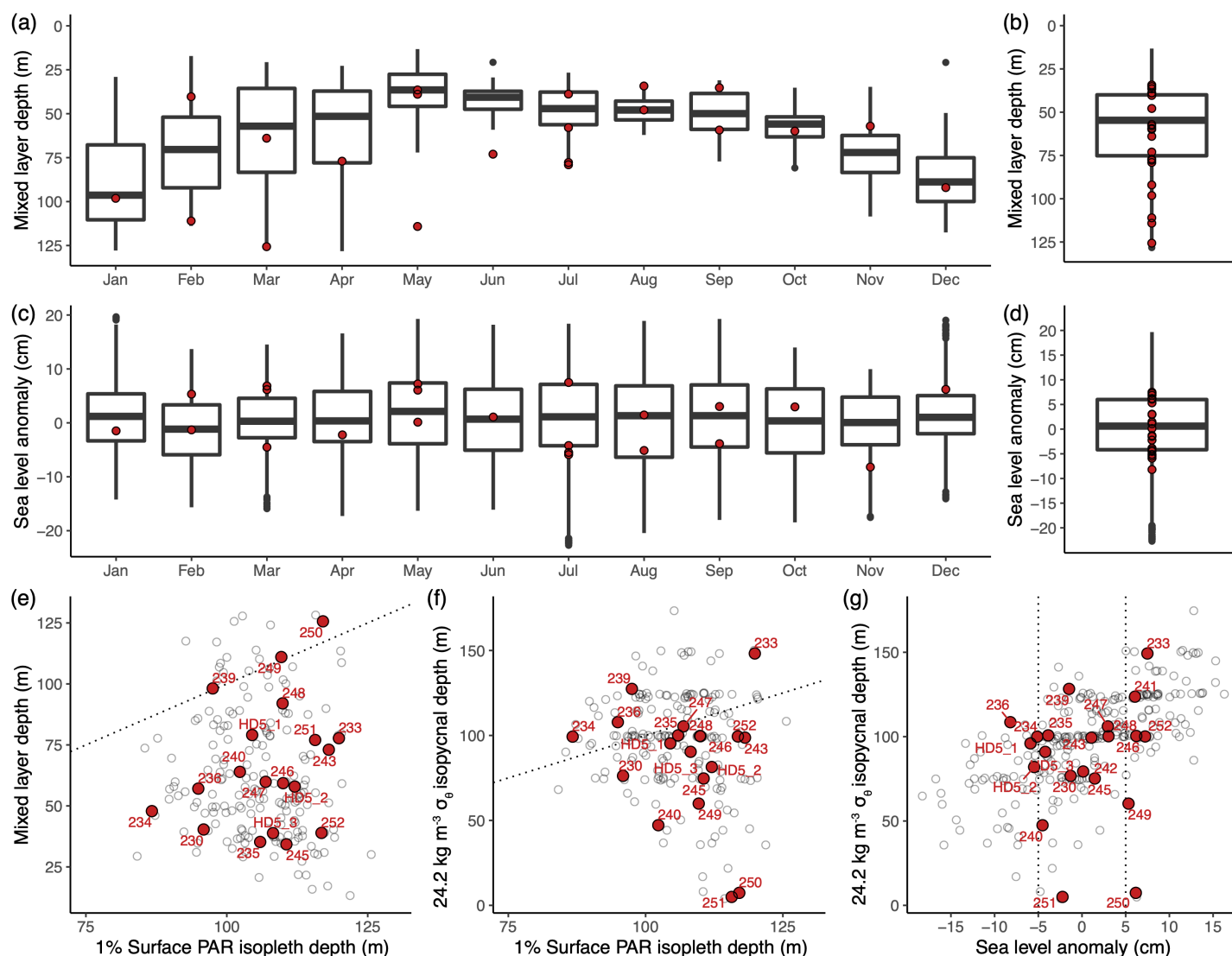
Fig. 2. Mixed layer depth and SLA$_{corr}$ highlight disturbance events in the context of HOT climatology. Calculated mixed layer depths of all HOT cruises from 1988 to 2019 **(a)** binned by month and **(b)** combined. SLA$_{corr}$ of all HOT cruises from 1993 to 2019 **(c)** binned by month and **(d)** combined. Relationships between the 1% surface PAR isopleth and the **(e)** mixed layer depth, and the **(f)** 24.2 kg m^{-3} σ$_\theta$. **(g)** Relationship between the 24.2 kg m^{-3} σ$_\theta$ and SLA$_{corr}$, with dashed lines marking when SLA$_{corr}$ ≤ −5.0 cm and SLA$_{corr}$ ≥ 5.0 cm. For **(a–g)**, red circles indicate samples collected during our time series (2011–2013). For **(e–g)**, samples collected during other HOT cruises are noted by gray open circles. For each boxplot, the median is indicated by the dark horizontal line, and box borders depict the 1st (Q1; 25th percentile) to the 3rd quartile (Q3, 75th percentile), with the whiskers extending to the maximum (Q3 + 1.5*[Q3 − Q1]) and minimum (Q1-1.5*[Q3 − Q1]).

photosynthetic picoeukaryotes were in general greater in the upper (0–75 m) euphotic zone than in the lower (100–175 m) euphotic zone, with highest abundances observed during February and March 2013 (H249 and H250; Table 1).

Quantification of disturbances

Disturbances were defined based on physical forcing of the upper ocean which were expected to alter light availability and nutrient supply. We considered disturbances attributable to both seasonal (convective mixing) and episodic (mesoscale) events. We observed 3 (January 2012 H239, February 2013

H249, and March 2013 H250) out of 22 total sampling occasions when the mixed layer depths deepened to below 1% surface PAR isopleth during the cruise (Fig. 2e). Retrospective analyses of HOT program observations revealed 17 such disturbances (approximately 10% of all cruises) for the period when both downwelling light and mixed layer depths have been measured (1998–2019), all occurring in the late winter or early spring. We also identified nine episodic mesoscale disturbances during our study period: three cruises (August 2011 H234, November 2011 H236, and July 2012 HD5) occurred when SLA$_{corr}$ ≤ −5 cm, and six cruises (July 2011 H233, April

2012 H241, December 2012 H248, February 2013 H249, March 2013 H250, and May 2013 H252) occurred when SLA$_{corr}$ ≥ 5 cm (Fig. 2g). Variability in SLA$_{corr}$ generally reflected temporal variability in the depth of the pycnocline (defined here as where $\sigma_\theta = 24.2$ kg m^{-3}) with a relatively constant 1% surface PAR isopleth (Fig. 2f), providing confidence that variations in SLA$_{corr}$ lend insight into vertical displacements of the pycnocline with respect to upper ocean light fields. Retrospective examination indicated 54 total occasions out of the 270 (20%) HOT cruises conducted since 1993 where SLA$_{corr}$ was < −5 cm, and 24.2 kg m^{-3} σ_θ was shallower than the 1% surface PAR isopleth in 34 of those occasions.

Vertical structuring of picoeukaryote community

The picoeukaryote community demonstrated strong vertical structure (Supporting Information Fig. S3c), with depth-specific alpha diversity (e.g., Shannon index and Chao1) remaining relatively constant through the well-lit euphotic zone (< 75 m), and decreasing and becoming more variable at deeper depths (100–175 m; ANOVA, $p = 1.9 \times 10^{-10}$; Supporting Information Fig. S3a). OTU richness, based on the Chao1 metric, increased somewhat in the mid-euphotic zone (75–100 m; ANOVA, $p = 2.2 \times 10^{-6}$; Supporting Information Fig. S3b). Beta diversity comparisons (Bray–Curtis dissimilarity) showed that communities became more dissimilar, relative to the near-surface waters, with increasing depth. Greater temporal variability was observed at depths between 75 and 175 m, consistent with more frequent disturbances observed in the lower regions of the euphotic zone (Supporting Information Fig. S3d).

Relative abundances of picoeukaryote taxa varied with depth, with specific taxa dominant in different regions of the upper ocean (Fig. 3 and Supporting Information Fig. S4a). Differentially abundant taxa across the upper and lower regions of the euphotic zone included picoeukaryotes from 26 taxa, including organisms such as Chrysophyceae, Dictyochophyceae, and Prymnesiophyceae that were most abundant in the upper euphotic zone, as well as organisms belonging to Acantharea, Mamiellophyceae, Pelagophyceae, and Polycystinea that tended to be more abundant at depth (Fig. 3). OTUs related to the Syndiniales displayed notable depth segregation, with approximately half of the population being more differentially abundant in the upper euphotic zone and the other half in the lower euphotic zone (Fig. 3). Relative abundances of specific OTUs occasionally demonstrated large changes (up to 10-fold) in the upper ocean (Fig. 3). For example, Pelagophyceae, which typically displayed highest abundances at 125 and 150 m, increased in relative abundance in the upper 75 m of the euphotic zone in January 2012 (H239) and March 2013 (H250) when mixed layer depths exceeded the 1% surface PAR isopleth (Figs. 3, 7a, Supporting Information Fig. S4b). Such seasonal scale increases of taxa typically found in the lower euphotic zone were also observed among the Mamiellophyceae,

Radiolaria, and Syndiniales. The opposite pattern was also observed, where taxa typically residing in the upper euphotic zone (e.g., Chrysophyceae, Dinophyceae, MAST-3, MAST-4, Prymnesiophyceae, Trebouxiophyceae, and Syndiniales) increased in relative abundance at depth during spring and winter months (Fig. 3).

Seasonality and mixing

To explore potential drivers of seasonal and vertical differences in picoeukaryote community structure, we compared communities within the euphotic zone using Bray–Curtis dissimilarities (Fig. 4). NMDS analyses of picoeukaryote communities revealed apparent seasonality in the upper euphotic zone (25 m), with samples from the spring and winter clustering more closely together than those from the summer and fall (Fig. 4a). In contrast, picoeukaryote communities in the lower euphotic zone (150 m) did not demonstrate clear seasonal variations (Fig. 4b). These patterns were confirmed by within-depth comparisons of picoeukaryote communities at 25 and 150 m. Pairwise comparison of all communities collected at 25 m relative to a community collected in March 2012 (H240) revealed seasonal scale modification in community structure (Fig. 4d); in contrast, pairwise comparisons for samples collected at 150 m revealed no clear seasonal variation in community structure and overall higher dissimilarity (> 0.55) throughout the year (Fig. 4e). Environmental controls on picoeukaryote communities revealed that while seasonality explained ~25% of variability in community structure for both upper and lower euphotic zones, change in SLA$_{corr}$ was a more significant control on picoeukaryote communities at 150 m (10%) compared to those at 25 m (5%, Appendix S1). These results suggest picoeukaryote communities in the upper and lower euphotic zones are controlled by varying processes operating over different timescales.

We further examined how variations in the mixed layer depth influenced vertical distributions of picoeukaryotes based on Bray–Curtis dissimilarity. We compared a representative mixed layer community (25 m) within a given depth profile against the community composition at all other depths sampled from that same vertical profile. For five representative depth profiles, communities within the mixed layer were more similar (~0.25 Bray–Curtis dissimilarity) to each other than communities below the mixed layer, implying mixing-driven vertical homogenization of picoeukaryote communities (Fig. 5a). Furthermore, photosynthetic picoeukaryote cell abundances and N + N concentrations also appeared to be influenced by mixed layer depth, with cell abundances remaining constant within the mixed layer (Supporting Information Fig. S5). In instances when the mixed layer was shallower than the 1% surface PAR isopleth, the 1% surface PAR coincided with the top of the nitracline and the DCML where highest picoeukaryote cell abundances were observed; however, in those instances when the mixed layer extended past the 1% surface PAR isopleth (e.g., H250), cell abundances
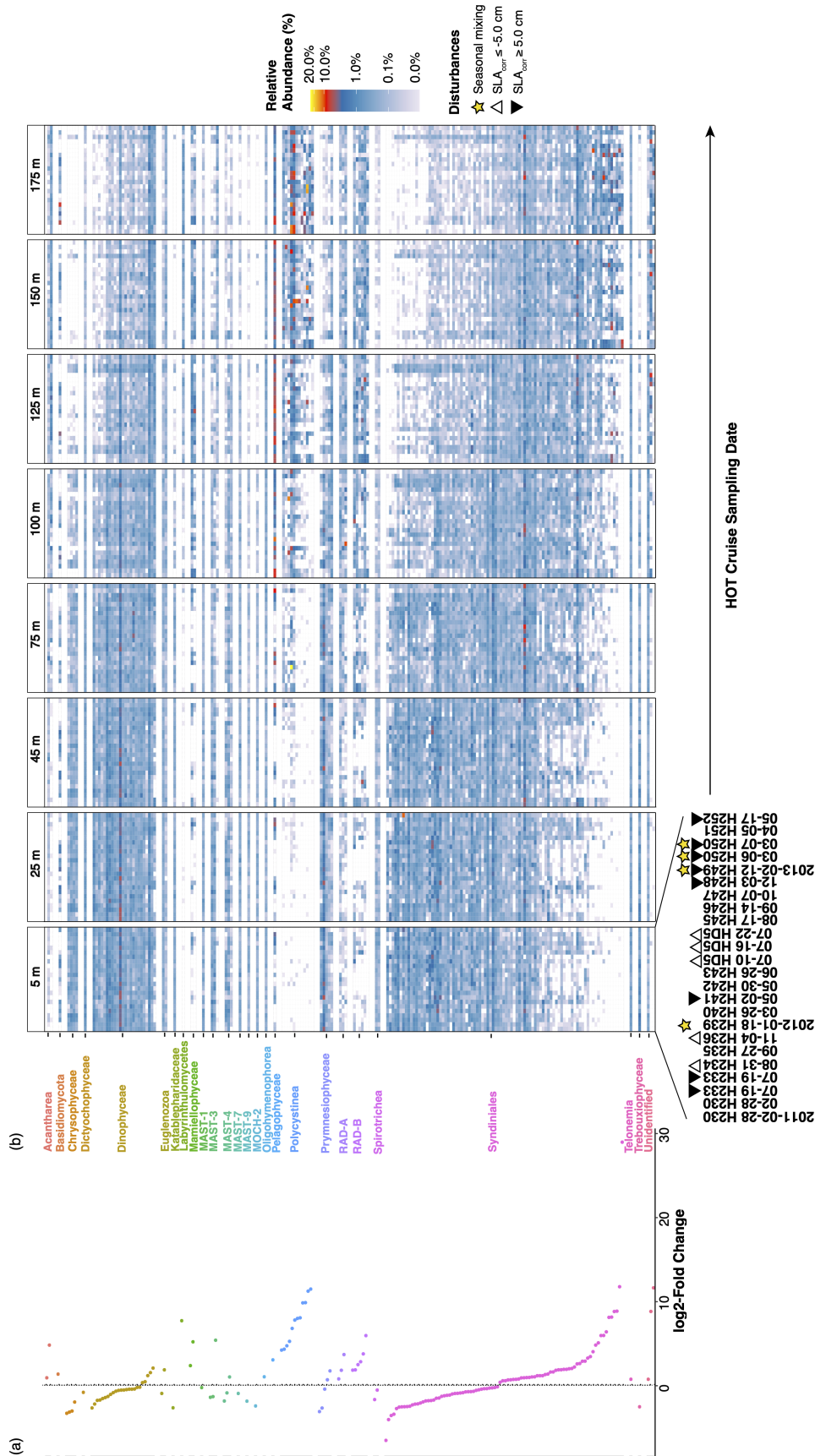
Fig. 3. Picoeukaryote OTUs are vertically structured within the water column and reveal temporal variability. **(a)** Enrichment of each differentially abundant OTU based on log2-fold change, with OTUs enriched in the upper euphotic zone (5–75 m) shown to the left of 0, and those enriched in the lower euphotic zone (100–175 m) shown to the right of 0. **(b)** Relative abundances of all differentially abundant OTUs in upper (5–75 m) and lower (100–175 m) regions of the euphotic zone, binned by the depth sampled and organized chronologically by the HOT cruise sampled. Each OTU is grouped at the class level, and the x-axis for each panel indicates dates DNA samples were taken, except for 5 m which is missing a sample from January 18, 2012 (H239). Markings for seasonal mixing events (yellow stars) and episodic mesoscale events when cruise-averaged SLA$_{corr}$ ≤ −5.0 cm (open triangles) and SLA$_{corr}$ ≥5.0 cm (black triangles).
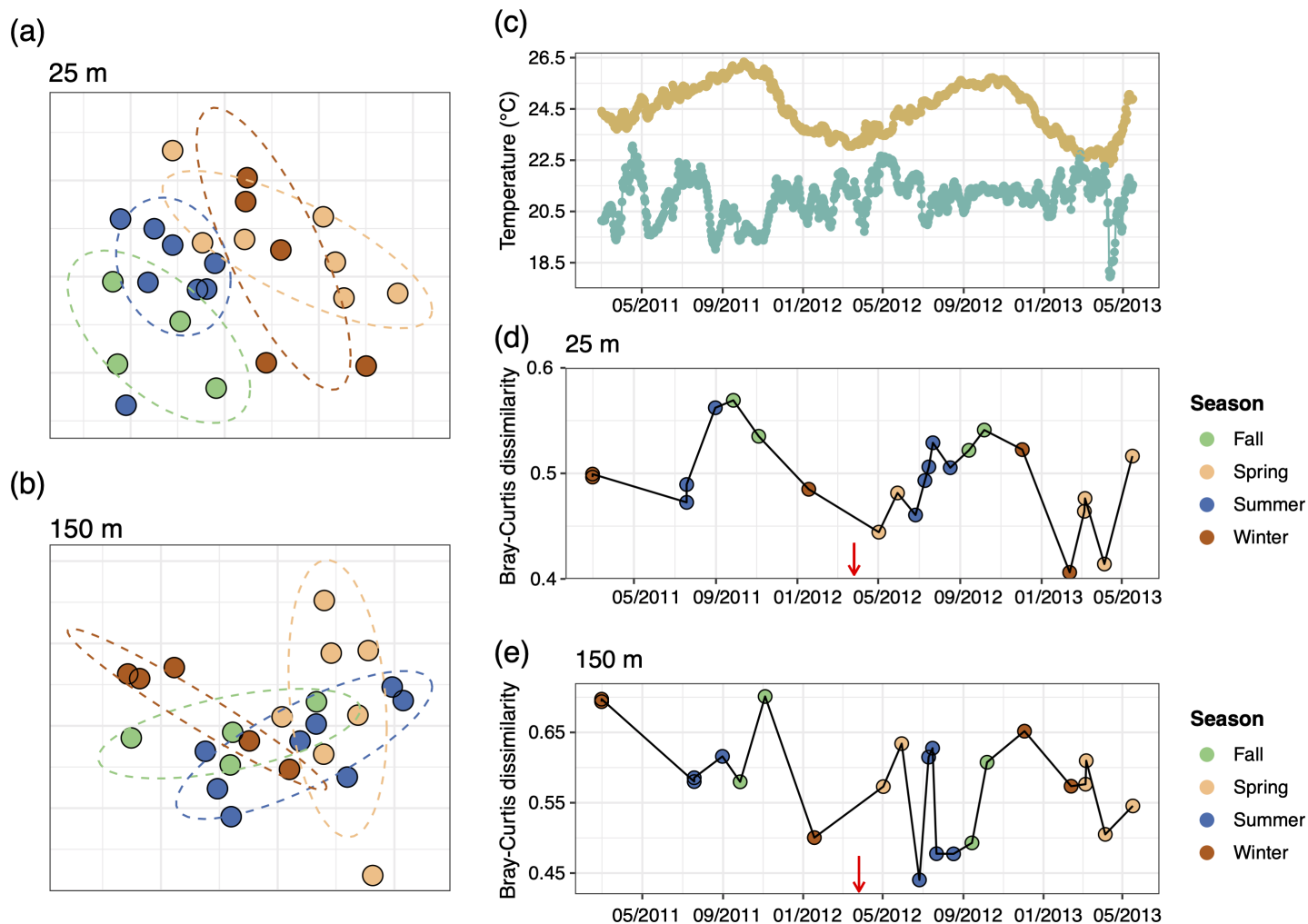
Fig. 4. Picoeukaryotic communities at different depths show varying responses to seasonal variability. NMDS of samples collected at **(a)** 25 m (stress = 0.17) and **(b)** 150 m (stress = 0.10), colored and grouped by season. **(c)** High-frequency (2 Hz) temperatures measured on the WHOTS mooring at 25 m (yellow) and 155 m (green). Bray–Curtis dissimilarity depicting pairwise comparison of samples collected on 26 March 2012 (H240, red arrow) against all other samples collected at **(d)** 25 m and **(e)** 150 m.

appeared homogenous down to the 1% surface PAR isopleth (Supporting Information Fig. S5). To determine if community composition varied seasonally due to deepening of the mixed layer, communities from 25 m were compared with all other samples collected within the same season. Comparisons of communities at 5 and 45 m against the 25 m depth horizon displayed similar dissimilarities (between 0.25 and 0.5 Bray–Curtis dissimilarity) regardless of season (Fig. 5c), consistent with these depths being perennially within the mixed layer. In contrast, the 25 m community appeared to be more similar (lower Bray–Curtis dissimilarity) to communities at 75 m only during spring and winter, when this depth resided within the mixed layer. Comparisons of the 25 m community to communities 100 m and deeper revealed them to be more similar during spring compared to other seasons, presumably due to more frequent occurrences of deeper mixed layers resulting in

physical homogenization of the typically stratified communities.

For further insight into the mixing-driven controls on vertical distributions of picoeukaryote communities, we examined a period (February to March 2013) during our observations when the mixed layer was anomalously deep relative to the HOT climatology. Our relatively short time series (2011–2013) coincided with periods when Station ALOHA experienced several occasions of anomalously deep mixing (Fig. 2a,b). We leveraged high-frequency (minute to hourly scale) measurements of temperature and salinity from the WHOTS mooring, together with daily scale estimates of SLA$_{corr}$, for insight into short-term (daily to weekly) physical forcing associated with these deep mixing events. These higher frequency observations provided historical context on physical disturbances that preceded our shipboard sampling of picoeukaryote
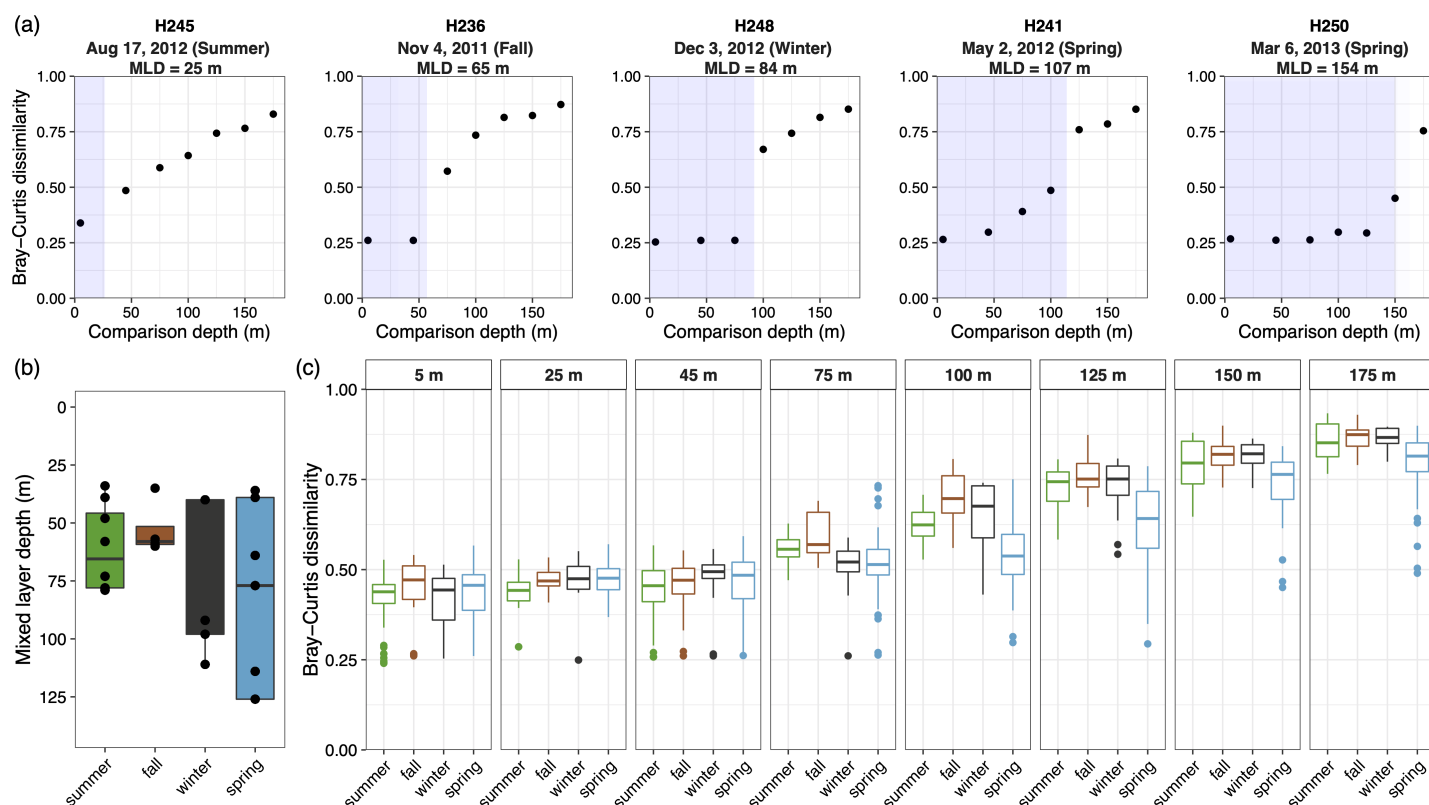
Fig. 5. Seasonal changes in mixed layer depth influence picoeukaryotic community structure. **(a)** Bray–Curtis dissimilarity of five different vertical profiles; plots are pairwise comparisons of community sampled at 25 m against other depths from the same vertical profile. The gray box represents the mixed layer depth of the specific cast when picoeukaryotic community sample was collected. **(b)** Cruise-averaged mixed layer depths grouped by season. **(c)** Bray–Curtis dissimilarity depicting pairwise comparisons of picoeukaryote communities sampled at 25 m against communities from other depths within the same season. Season colors are the same as in (b). For each boxplot, the median is indicated by the dark horizontal line, and box borders depict the 1st (Q1; 25th percentile) to the 3rd quartile (Q3, 75th percentile), with the whiskers extending to the maximum (Q3 + 1.5*[Q3 − Q1]) and minimum (Q1-1.5*[Q3 − Q1]).

communities. Here, we focus on two sampling events that occurred during back-to-back HOT cruises in February (H249) and March 2013 (H250), to describe how leveraging information on the time history of physical disturbances aided our understanding of plankton community resilience.

During February 2013 (H249), the mixed layer depth varied between 46 and 164 m over the course of the 4-day sampling period, suggesting substantial submesoscale spatial variability within and around Station ALOHA (Supporting Information Fig. S6). The mixed layer depth on the cast we collected samples for picoeukaryote DNA (12 February) was 56 m. Consistent with this, our analyses of Bray–Curtis dissimilarity suggested picoeukaryote communities within the mixed layer differed from those below the mixed layer (Fig. 6b). We used mooring-based temperature and salinity measurements to examine physical dynamics immediately prior to our shipboard sampling, which revealed that in the days prior to our sampling (10–11 February), the upper ocean experienced a short-period isopycnal uplift, reflected as decreases in temperature and salinity through the lower euphotic zone (95–155 m; Figs. 6a, Supporting Information Figs. S7, S8). Following this

short-duration event, isopycnal surfaces appeared to relax, with subsequent reestablishment of the thermocline between 100 and 135 m. The resulting upward displacement of cold water during this event was limited in duration to a ~12-h period between 10 and 11 February (Fig. 6). Such punctuated uplift in isopycnal surfaces would be expected to vertically introduce nutrient-enriched waters into the euphotic zone, potentially stimulating plankton growth. However, our shipboard sampling on 12 February coincided with the period where isopycnal surfaces had relaxed, and the mixed layer was beginning to vertically expand (as evidenced by the deepening mixed layer throughout the cruise). Hence, our sampling captured the short window of time between a punctuated isopycnal uplift event and a deepening mixed layer. In this case, the vertically stratified picoeukaryote community provides insights into rapid time-scales of the community response to such spatially heterogeneous physical disturbances to the euphotic zone.

In March 2013 (H250), we sampled one of the deepest mixing events ever recorded at Station ALOHA. Similar to conditions during H249, the mixed layer depth was highly
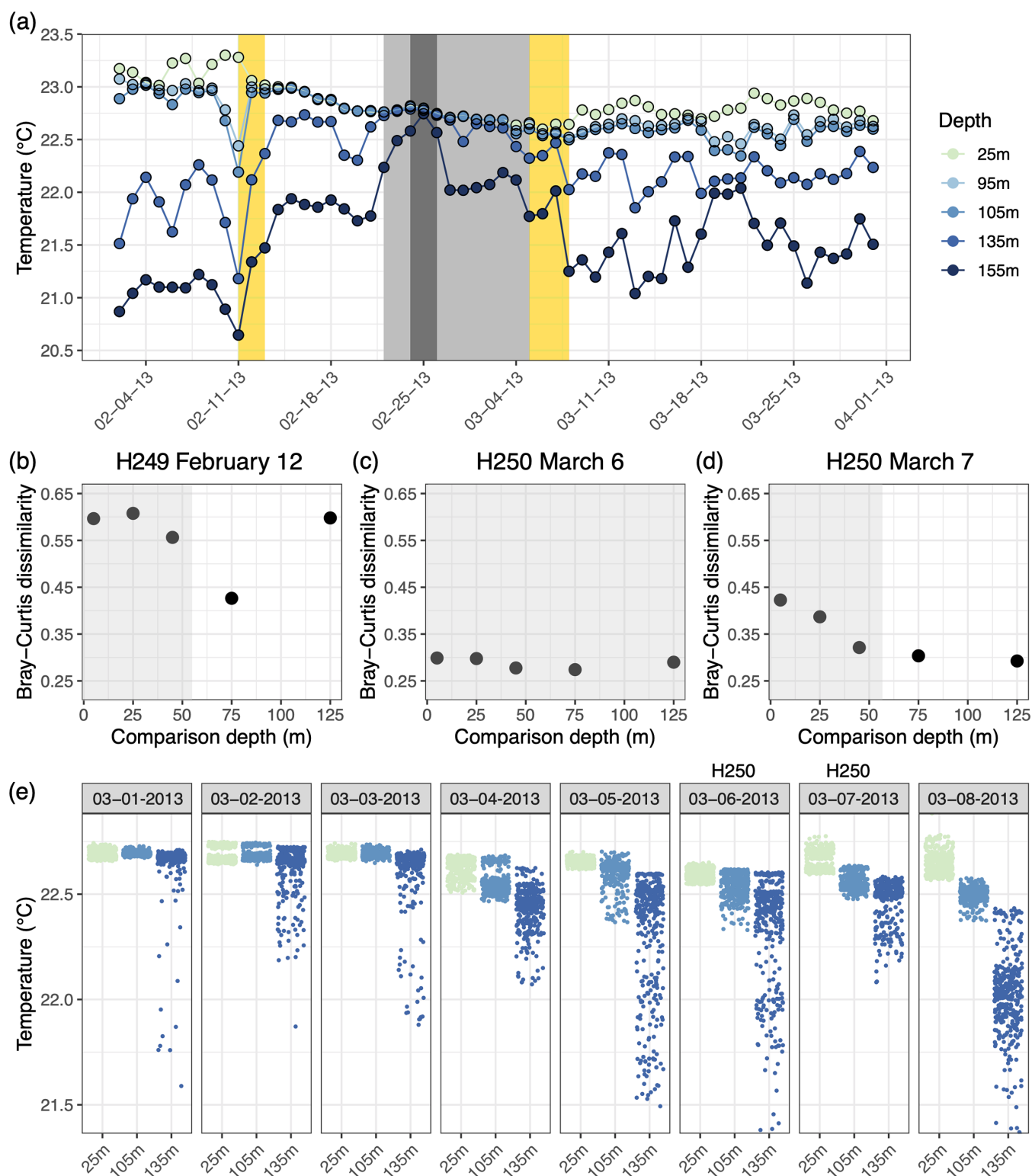
Fig. 6. Picoeukaryotic communities respond on daily-to-weekly timescales after an anomalous deep mixing event. (**a**) WHOTS mooring-based daily temperature measurements at 25, 95, 105, 135, and 155 m; yellow bars represent the days where picoeukaryote sampling occurred (12 February 2013 for H249, 06 March 2013 and 07 March 2013 for H250), wide light gray bar indicates where upper ocean temperatures appear homogenized to nearly 135 m, and dark gray bar depicts where temperatures appear to homogenize down to 155 m. (**b, c, d**) pairwise comparisons, based on Bray–Curtis dissimilarity, of picoeukaryote communities; communities at discrete depths from H249 and two discrete profiles on H250 are compared relative to the 100 m community. Light gray squares indicate communities within the mixed layer. (**e**) Variations in seawater temperature measurements at 25, 95, and 105 m from WHOTS mooring from 01 March 2013 to 08 March 2013.

variable over the course of this 4-day cruise (varying between 16 and 164 m; Table 1, Supporting Information Fig. S6). The WHOTS mooring provided a robust time series record documenting the interaction of spatial heterogeneity and seasonal-scale modification of the upper ocean. The daily-averaged mooring-based temperature and salinity measurements revealed that approximately 10 d prior to our shipboard sampling on 06 March, the mixed layer penetrated to at least 155 m (Figs. 6a,e, Supporting Information Fig. S9). Three days later, the mixed layer began to shoal, with temperatures through the upper 105 m warmer than those at 135 and 155 m (Fig. 6a). On 05 March 2013, one day prior to the period of our shipboard sampling, temperatures in the upper 45 m began to show signs of stratification, continuing to progress through the HOT shipboard occupation of Station ALOHA (Fig. 6e). Our sampling for picoeukaryote community structure over two consecutive days (06 and 07 March) captured this period of deep mixing and subsequent onset of stratification. On 06 March, despite evidence that upper ocean temperature structure had begun to restratify following the deep mixing event, Bray–Curtis dissimilarity analyses revealed that the picoeukaryote community remained vertically homogenized down to 125 m (Fig. 6c). Taxa which were typically observed at shallower depths were present in higher abundances as deep as 175 m (Fig. 3b), consistent with a mixed layer which had previously exceeded 155 m (e.g., on 25 February). However, 1 d later (07 March), the mixed layer depth shoaled to ~57 m and communities in the well-lit upper ocean demonstrated increasing dissimilarity relative to the deeper communities (Fig. 6d). These results provide unique insight into timescales of picoeukaryote community response to spatially and temporally variable mixing disturbances, with the resulting timescales of apparent picoeukaryote resilience in the upper ocean of approximately 1 week.

Episodic disturbances

We also examined disturbances due to vertical fluctuations in the pycnocline, such as those attributable to temporal and spatial perturbations stemming from mesoscale physics. We defined such disturbances as when SLA_{corr} was ≥ 5.0 cm and ≤ −5.0 cm, consistent with Barone et al. (2019) who identified such conditions as imparting distinct biogeochemical signatures on the upper ocean at Station ALOHA. In order to examine picoeukaryote community response to changes in SLA_{corr}, we examined relative abundances of Pelagophyceae and Polycystinea, which are found almost exclusively in the lower euphotic zone (and deeper for Polycystinea; Ollison et al. 2021). Hence, vertical displacement of isopycnals would be expected to disrupt their depth distributions. Consistent with this expectation, OTUs related to the Pelagophyceae, typically most abundant between 100 and 150 m, increased in relative abundance at shallower depths when SLA_{corr} was ≤ −5.0 cm (August 2011, November 2011, and July 2012; Fig. 7a,c). When communities were grouped based on events

when SLA_{corr} > 0 cm or SLA_{corr} < 0 cm, differences in Pelagophyceae relative abundances were significantly different at 100 m depending on SLA_{corr} (t-test, $p < 0.03$). Similarly, OTUs related to the Polycystinea typically found at 175 m showed periodic fluctuations in relative abundances at shallower depths, coincident with the shoaling of isopycnal surfaces during periods when SLA_{corr} was ≤ −5.0 cm (Fig. 7b, d). Differences in Polycystinea relative abundances as a function of SLA_{corr} were significant at 125 and 175 m when grouped by SLA_{corr} > 0 cm or SLA_{corr} < 0 cm (t-test, $p < 0.04$). Few occasions when SLA_{corr} was ≥ 5.0 cm (February and March 2013) coincided with deep mixing events; on these occasions, Pelagophyceae appeared entrained into the upper euphotic zone (Fig. 7a).

During the summer of 2012, we collected samples for subsequent analyses of picoeukaryote community structure on five separate occasions over a ~5-week period. At the beginning of this more intensive shipboard sampling campaign (26 June), SLA_{corr} was weakly positive (1 cm; Fig. 8b). However, by the following sampling period (10 July), SLA_{corr} had decreased to −6 cm, coincident with uplift of cooler water into the lower euphotic zone (as reflected based on the WHOTS temperature record; Fig. 8a,b). Mixed layer temperatures remained unaffected by this event, with temperatures in the near-surface ocean (5 m) demonstrating seasonal warming (Fig. 8a). The uplift of cooler waters into the lower euphotic zone coinciding with SLA_{corr} ≤ −5.0 cm indicates a mesoscale feature passed through Station ALOHA during this focused summer sampling period (Fig. 8b). This disturbance appeared most intense between 26 June and 10 July, and resulted in initial decreases in temperature and increases in N + N concentrations in the lower euphotic zone, consistent with isopycnal uplift (Fig. 8b–d). Picoeukaryotic community structure appeared to respond to the passage of this feature, with NMDS analyses for the lower euphotic zone demonstrating marked differences in community composition between 26 June and 10 July (Fig. 4e, Fig. 8c,d). Coincident with the period of isopycnal uplift, picoeukaryote taxa typically found deeper in the euphotic zone demonstrated elevated relative abundances; for example, Polycystinea increased significantly in relative abundance over this time period (Fig. 8e). Approximately 1 week later (16 July 2012), temperatures in the lower euphotic zone had warmed and N+N concentrations had decreased, reflecting the relaxation of isopycnal surfaces that had previously been displaced upward with consumption of N+N along those surfaces. NMDS analyses revealed that the picoeukaryote community structure was distinct from the previous sampling 1 week earlier, yet remained very different from the initial community sampled in late June (Fig. 8c–e). Approximately 1 week later (22 July), the community in the lower euphotic zone (150 m) shifted again, this time becoming increasingly similar in structure to the community sampled prior to the onset of this event (Fig. 8c,d). Throughout this entire period, no change in temperature, N+N, and community
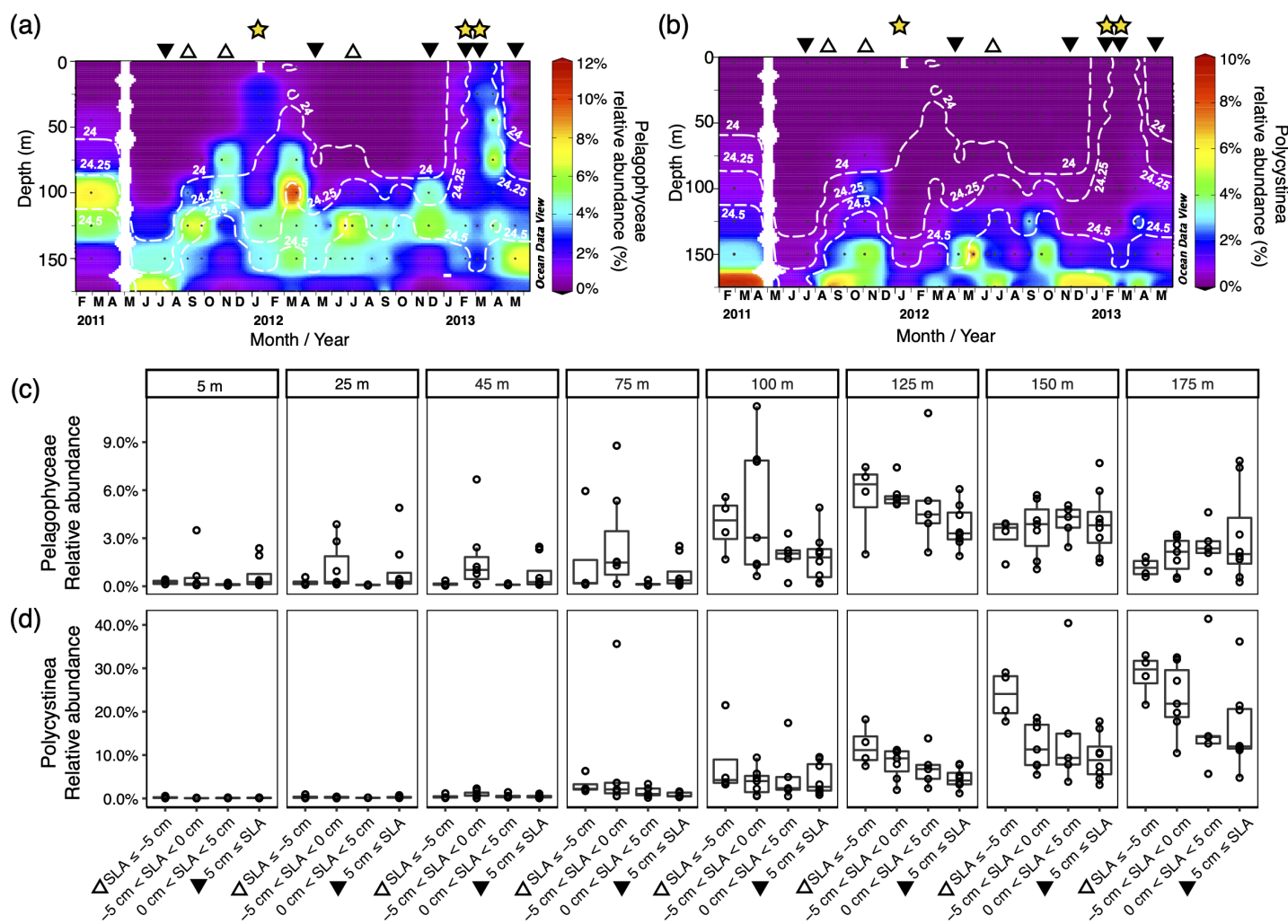
Fig. 7. Lower euphotic zone-associated lineages are more abundant at shallower depths when SLA$_{corr}$ is negative. Contour plots depicting relative abundances of **(a)** Pelagophyceae *Pelagomonas calceolata* and **(b)** Polycystinea Spumellarida group I during this study. Isopycnal surfaces (kg m^{-3}, σ_θ) are overlaid on each plot (white dashed lines) and black circles indicate depths of sample taken. Variability in relative abundances of **(c)** all Pelagophyceae OTUs and of **(d)** all Polycystinea OTUs binned based on periods of either negative or positive SLA$_{corr}$ and arranged by depth. Note scale differences in relative abundance for each panel. Seasonal mixing events (yellow stars), and episodic mesoscale events when cruise-averaged SLA$_{corr}$ ≤ −5.0 cm (open triangles) and SLA$_{corr}$ ≥ 5.0 cm (black triangles) are marked. For each boxplot, the median is indicated by the dark horizontal line, and box borders depict the 1st (Q1; 25th percentile) to the 3rd quartile (Q3, 75th percentile), with the whiskers extending to the maximum (Q3 + 1.5*[Q3 − Q1]) and minimum (Q1 − 1.5*[Q3 − Q1]).

composition in the upper euphotic zone (25 m) was apparent, indicating the influence of this feature was isolated to the lower euphotic zone (Supporting Information Fig. S10).

Discussion

Results from this study suggest that in the face of physical disturbances, including deep mixing events and vertical displacement of the pycnocline, euphotic zone picoeukaryotic communities in the NPSG were relatively resilient, recovering on daily to weekly timescales. Unfortunately, our Eulerian time series does not allow disentangling biological responses to discrete disturbances from movement of physically and

biologically distinct water masses through the Station ALOHA sampling region. However, our observations highlight the role of submesoscale and mesoscale physical processes in modifying distributions of plankton, and emphasize that such episodic events are superimposed on seasonal-scale modification of the upper ocean. We observed that although mixing events vertically homogenized distributions of picoeukaryote taxa including entraining picoplankton typically restricted to the lower euphotic zone into the well-lit upper ocean and vice versa, these communities rapidly reorganized to their prior vertically structured state within days following the onset of stratification. In the lower euphotic zone, fluctuations in the pycnocline attributable to mesoscale physical disturbances
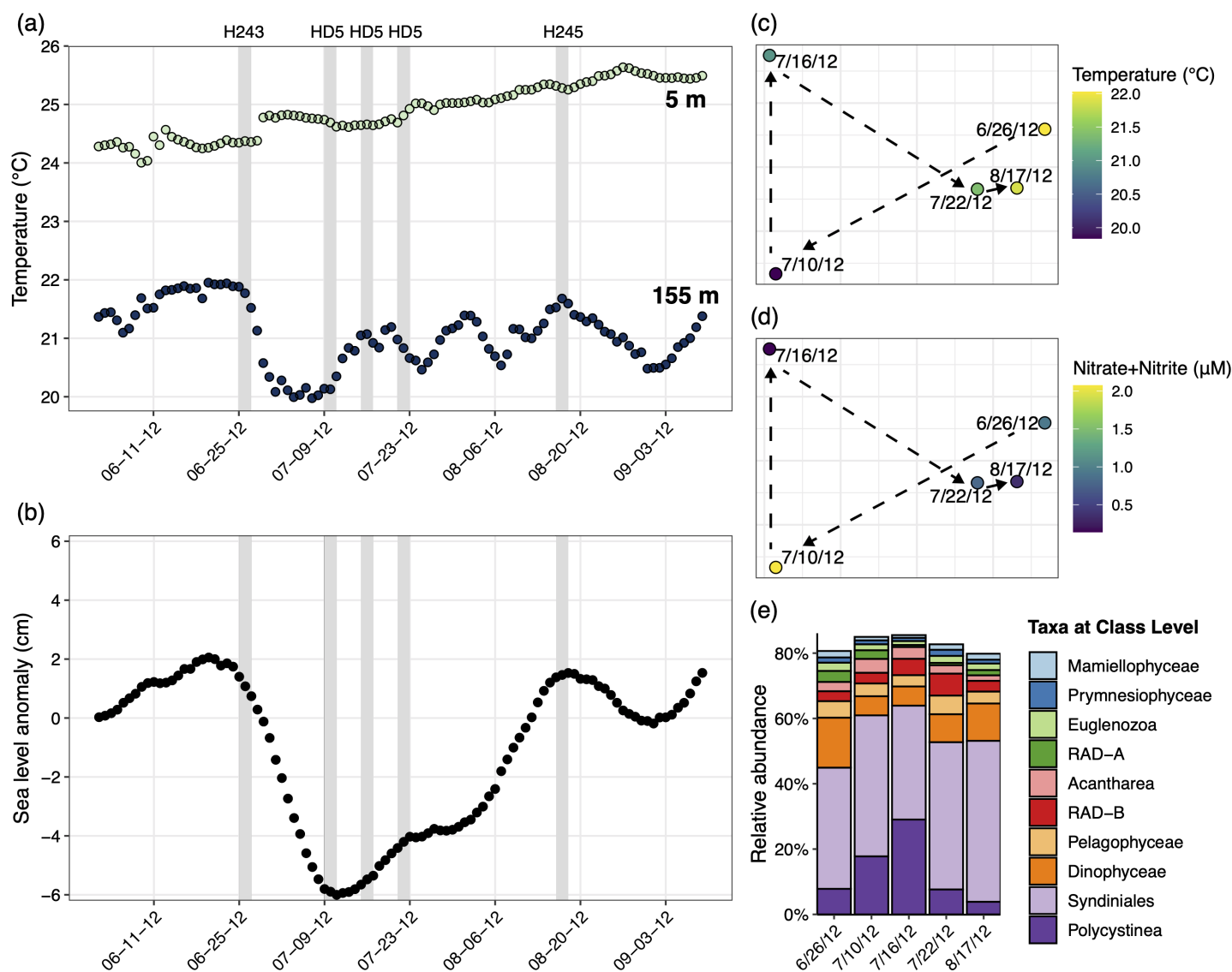
Fig. 8. Picoeukaryotic communities respond on weekly-to-monthly timescales to an anomalous SLA event moving through Station ALOHA. **(a)** Daily-averaged WHOTS mooring-based temperatures at 5 and 155 m, and **(b)** SLA$_{corr}$, from June to September 2012, encompassing five sampling periods (indicated by gray bars, on 26 June, 10 July, 16 July, 22 July, and 17 August, from H243, HD5, and H245). NMDS depicting similarities of 150 m picoeukaryote community composition colored by **(c)** temperature and **(d)** N+N concentrations from 26 June 2012 to 17 August 2012. **(e)** Time-varying changes in the relative abundances of picoeukaryote taxa (150 m) at class level from 26 June 2012 to 17 August 2012.

altered the vertical distributions and relative abundances of picoeukaryote taxa. Again, following these events, the picoeukaryote community structure recovered on daily to weekly timescales. Thus, irrespective of the form of disturbance, our time series sampling revealed that picoeukaryote communities in both the well-lit and the dimly lit regions of the euphotic zone were resilient, often on timescales faster than our approximately monthly scale sampling. Whether such biological reorganization reflects the balance of plankton growth and removal processes or stems from vertical or horizontal redistribution of organisms due to submesoscale spatial variability remains unresolved by our observations, but disentangling these dynamics is central to

improving our understanding of the stability of this ecosystem (Lévy et al. 2018).

Plankton resilience based on seasonal-scale dynamics of disturbance in the NPSG

Strong vertical gradients in light energy, nutrient concentrations, and seawater density promote vertical partitioning among plankton communities in the NPSG (Venrick 1993; Ollison et al. 2021). We hypothesized that deep mixing events would act as disturbances by reducing light available to support plankton growth in the upper ocean and disrupting the vertical structure of depth-segregated communities. Seasonal-

scale changes in light energy, due to mixing and stratification dynamics, have long been considered as key determinants on plankton productivity (Sverdrup 1953). We predicted such mixing and stratification dynamics would also impact the vertical distributions and relative abundances of plankton. Throughout our study, seasonal mixing variability was consistent with the HOT program climatology (Karl and Church 2014); however, we observed large variations in the depths of the mixed layer during our entire sampling period at Station ALOHA. Our time series of picoeukaryote communities revealed that in the well-lit region of the euphotic zone, the composition of picoeukaryote communities demonstrate modest seasonal fluctuations, with communities becoming increasingly dissimilar (relative to the summer) during periods of destratification and deepening of the mixed layer. Our amplicon time series data provide examples of apparent mixing entrainment of taxa that are typically relegated to the dimly lit waters into the upper euphotic zone, and mixing-driven vertical redistribution of upper euphotic zone taxa to depths outside their typical range.

Seasonal patterns in plankton community composition coincident with convective mixing have been previously documented (Giovannoni and Vergin 2012; Choi et al. 2020), revealing highly adapted organism structure and successional patterns. Previous analyses at Station ALOHA revealed that microorganism community structure is sensitive to wind-driven forcing of the upper ocean; Bryant et al. (2016) observed a correlation between alpha diversity and wind speeds 3 to 10 d prior to sample collections, suggesting tightly coupled biological responses to wind-induced turbulent mixing. Persistence of taxa that typically reside at depth in the euphotic zone (e.g., Pelagophyceae) during periods of deeper mixing may reflect the ability of these taxa to rapidly adapt to variable light conditions through xanthophyll cycling (Dimier et al. 2009; Bidigare et al. 2014). Choi et al. (2020) observed notable increases in pelagophytes in the surface waters as well as in the DCML where they are typically found, during seasonal deep mixing in the western North Atlantic, and speculated that they rely on nitrate as a primary nitrogen source. During March 2013 (H250), deep mixing that occurred days prior to our sampling appears to have vertically redistributed N+N in the euphotic zone (Supporting Information Fig. S5a), which may have entrained Pelagophyceae into the upper euphotic zone, but also increased their growth rates through the availability of nutrients in the upper euphotic zone. Conversely, redistribution of upper euphotic zone taxa like prymnesiophytes, chrysophytes, and MAST groups beyond their typical depth range may drive such taxa to rely more heavily on heterotrophic and/or mixotrophic physiologies (Hartmann et al. 2012), influencing food web dynamics throughout the euphotic zone. Whereas acquisition of nutrients via mixotrophy could confer competitive advantages to these taxa in the nutrient-limited upper euphotic zone at Station ALOHA, their physiologies and activities when distributed into relatively nutrient-rich regions are unknown and remain to be explored (Caron et al. 2017; Choi et al. 2020).

Examining high-frequency mooring-based temperature and salinity measurements during the deep mixing event in March 2013 (H250) allowed temporal contextualization of our observations on picoeukaryote community structure, including the short timescales (~3 d) of vertical reorganization of the community following the onset of stratification. While the communities were vertically distinct at depths exceeding the 125-m mixed layer depth, many taxa from the upper ocean persisted at 175 m, indicating these communities had not yet completely recovered from the deep mixing disturbance that occurred prior to H250. These rapid timescales of resilience are consistent with generation times for picoeukaryotes in the upper euphotic zone (ranging 0.6–1.3 d^{-1}; Worden et al. 2004, Rii et al. 2016). Interestingly, biomass-normalized production rates at Station ALOHA during the period of the current study indicate rates were greatest coincident with the March 2013 deep mixing event (Rii et al. 2016). Such findings suggest rapid picoeukaryote growth, in response to turbulent supply of nutrients coincident with increased incident light availability, may underlie the resilient response to one of the deepest recorded mixing events in the 30+ year shipboard time series record. In fact, it is possible that the distinct picoeukaryote communities in the winter and spring may allow them to rapidly capitalize on increased nutrients supplied through deeper mixing.

Event-scale dynamics of disturbance and variable timescale of resilience at NPSG

While the timescale of resilience among picoeukaryotes in the euphotic zone appears to be on the order of 1 week in response to seasonal deep mixing, the timescales of resilience to meso- to submesoscale events, whose impacts are largely restricted to the lower euphotic zone, appear somewhat longer, on the order of weeks to a month. Mesoscale dynamics appear to be key contributors to biological variability in the NPSG (Barone et al. 2019), as mesoscale eddies in this region vary in size, amplitude, rotational velocity, and polarity (Chelton et al. 2011). SLA$_{corr}$ has been widely used to detect and describe variability in the ocean pycnocline due to mesoscale physical dynamics such as eddies (e.g., McGillicuddy et al. 1998). Approximately 30% of historical (1992–2012) HOT program sampling at Station ALOHA appears influenced by the passage of mesoscale eddies, and approximately half of the variability associated with SLA$_{corr}$ in this region has been attributable to eddies (Barone et al. 2019). Consistent with previous studies (McGillicuddy et al. 1998; Church et al. 2009; Barone et al. 2019), we found that fluctuations in SLA$_{corr}$ correlated with variability in the depth of isopyncal surfaces positioned in the lower euphotic zone. Specifically, SLA$_{corr}$ explained ~40% of the variability in the depth of 24.2 kg m^{-3} σ_θ that typically intersects the DCM at Station ALOHA.

Variability in SLA$_{corr}$ at Station ALOHA has previously been linked to fluctuations in nutrient concentrations and stoichiometry, and variations in photosynthetic picoeukaryote abundances, particularly through the lower euphotic zone (Church et al. 2009; Ascani et al. 2013; Barone et al. 2019). Barone et al. (2019) found that across 23 years of observations (1993–2012), SLA$_{corr}$ at Station ALOHA varied between approximately −20 cm and 20 cm; in comparison, SLA$_{corr}$ varied between −8 cm and 8 cm during our study. Hence, our period of study appears to have coincided with a relatively quiescent period for mesoscale events at this site. Nonetheless, even with the relatively weak variation in SLA$_{corr}$, we found evidence that mesoscale dynamics have a demonstrable effect on vertical structure of picoeukaryote communities in the lower euphotic zone.

Mesoscale physical dynamics alter plankton communities in several ways, including through changes in the vertical positioning of the pycnocline and through physical reorganization of the habitat (e.g., stirring or mixing). Eddy-driven vertical heaving of isopycnal surfaces alters distributions of plankton and nutrients relative to gradients in sunlight; for example, changes in isopyncal surfaces attributable to cyclonic (McGillicuddy et al. 1998; Benitez-Nelson et al. 2007) and anticyclonic (Dufois et al. 2016) eddies have been shown to shift phytoplankton community structure in the euphotic zone. Eddies can also trap plankton communities, behaving as isolated vortices with the potential to horizontally transport biological communities (Chelton et al. 2011).

We conducted higher frequency (weekly scale) sampling from June to August 2012 (H243, HD5, H245), which coincided with one of the stronger SLA$_{corr}$ excursions during our study and provided unique insight into the resilience of the plankton community in response to mesoscale disturbances. In particular, we sampled the passage of an event that resulted in isopycnal uplift into the lower euphotic zone, as evidenced by intrusion of cooler, more nutrient-enriched waters into the lower euphotic zone. We saw evidence of shifts in picoeukaryote community in the lower euphotic zone over the course of several days during and after this event. We also saw evidence of a shift in picoeukaryote community that coincides with the period when nutrients supplied through isopycnal uplift are assimilated into plankton biomass, illustrating the rapid response capabilities of upper ocean plankton to this physical disturbance. As the cyclone moved through the sampling region, isopycnal uplift relaxed (as evident from both increasing SLA$_{corr}$ and seawater temperatures) and the picoeukaryote community began to resemble the predisturbed community. These findings are consistent with changes in physical properties, productivity, and increased picoeukaryote abundances at depth observed during this same time period at Station ALOHA (Wilson et al. 2015). A previous study at Station ALOHA that coincided with the period of the current study found rates of picoeukaryote biomass-normalized

production were time variable, but that rates in the lower euphotic zone were ~three-fold lower than those in the upper euphotic zone (Rii et al. 2016), consistent with observations here that time-scales of resilience in the lower euphotic zone appear somewhat longer than those due to mixing in the upper euphotic zone.

Eulerian perspectives on a spatially and temporally heterogeneous ocean

Since our study relied on Eulerian time series observations, our evaluation of resilience in this community cannot distinguish spatial variability associated with water transport from time-varying changes in plankton growth rates. Thus, it is difficult to disentangle whether our observations of resilience derive from planktonic growth and succession, or reflect spatial heterogeneity in community structure at the meso- and submesoscales. Chelton et al. (2007) estimated that mesoscale eddy diameters in the subtropical Pacific range from 100–200 km, and these features generally propagate westward with horizontal velocities of ~4–10 km d^{-1}. Hence, a 200-km eddy could take between 22 and 60 d to move completely through the Station ALOHA sampling region. Consistent with these estimates, Barone et al. (2019) found that the time for mesoscale eddies to propagate through Station ALOHA was approximately 1 month, consistent with our observations during the summer of 2012. In 1997, a cyclonic eddy passing by a mooring near Station ALOHA in March to April (H81 and H82) resulted in uplift of the nitracline and the DCML; however, by May of that year, all indications of any disruption to the biological community had disappeared, and there was no evidence of a significant increase in Chl *a* in the upper euphotic zone (Letelier et al. 2000). However, eddies demonstrate heterogeneity at submesoscales; eddy structure can vary from the center to edges (Lévy et al. 2018), and such spatial heterogeneity at submeso- and mesoscale is well-documented around Station ALOHA (Calil and Richards 2010) and apparent in our data. Vertical displacement of isopycnal surfaces resulting from internal waves, tidal forcing, and near-inertial period oscillations can displace the depth of the DCML on time-scales <1 d (Karl et al. 2003). Short-lived (< 2 months) nutrient pulses, such as described here, with effects in the lower euphotic zone, can alter local and regional scale plankton processes, with cumulative effects on community structure and biogeochemical cycles in the NPSG (Karl 2002).

We found that the spatiotemporal mosaic of physical disturbances are not mutually exclusive, such that mesoscale events, over and above seasonal changes in the depth of mixing and light, may define the emergent distributions and resilience of the euphotic zone picoeukaryote community. In the stratified, oligotrophic NPSG, mixing is generally restricted to the upper 60 m, with the 1% surface PAR isopleth residing between 84 and 125 m. We collected samples on two consecutive days (06 March 2013 and 07 March 2013) during H250 which revealed a shallowing of the mixed layer depth from

154 to 57 m after 1 d (Supporting Information Fig. S6). Such results likely reflect submesoscale spatial-scale heterogeneity in the habitat, where two physically distinct parcels of water were likely sampled on these different days. The Eulerian design of our study does not allow us to differentiate influences of spatial heterogeneity from those deriving from time-varying dynamics. At the submesoscale, biological response times overlap with timescales of the physical movement (spatially horizontally and possibly vertically) of water. For example, at an approximate net growth rate of 0.5 d^{-1} in the NPSG, the time for a population to double would be ~1.3 d. If a submesoscale feature, with a distinct biological community, advected through Station ALOHA at a rate of ~ 5 km d^{-1}, the resulting perturbation to the community and subsequent return to predisturbed state (resilience) would be less than 1 week, indistinguishable from the net biological response. Hence, although our study provides insights into variable time-scales of resilience of the picoeukaryote community to different forms of disturbance at Station ALOHA, whether that resilience derives from biological responses following disturbance (i.e., re-establishment of equilibrium in growth and removal) or reflects the return of biological structure following physical movement of organisms associated with advected water mass features through our sampling site remains unclear. Thus, a Lagrangian sampling design, where a specific meso- or submesoscale feature with its associated plankton dynamics can be tracked over time, would aid in understanding the mechanisms that underlie the resilient responses to disturbance observed in picoeukaryote community structure at Station ALOHA. Such a study, coupled with Lagrangian instruments such as ocean gliders and floats to attain high spatial and temporal frequency measurements of temperature and salinity, and satellite-derived measurements such as SLA_{corr}, would be required to assess recent history of disturbances and the varying timescales of response by the plankton community at Station ALOHA.

Conclusions

This study highlights that plankton communities in the NPSG are susceptible to disturbances that redistribute organisms relative to gradients in light and nutrients. Our results suggest the picoeukaryote community is relatively resilient to such physical disturbances, with postdisturbance community structure typically returning to resemble the predisturbance structure on daily to weekly timescales. The overlap in biological response times and timescales of submesoscale physical water movement makes it difficult to disentangle which of these mechanisms controls community structure based on the Eulerian observations from this study. However, this collective set of observations highlight a number of intriguing biological dynamics, including that the juxtaposition of mesoscale and submesoscale disturbances on more predictable seasonal succession patterns complicates assessment of community resilience. Seasonally variable patterns on succession present

moving targets with respect to identifying the time required for the community to respond and return to a predisturbed state following disturbances occurring at a higher frequency than seasonal scales. In addition, observations suggest that the duration, intensity, speed, and possibly the age of mesoscale physical dynamics influences eukaryote community resilience. We emphasize the importance of examining the near-time (days to weeks) history of disturbances for insights into contemporaneous plankton community structure. Such studies are relatively rare for the open ocean, largely as a result of the necessity for time-resolved observations.

References

Alexander, H., M. Rouco, S. T. Haley, S. T. Wilson, D. M. Karl, and S. T. Dyhrman. 2015. Functional group-specific traits drive phytoplankton dynamics in the oligotrophic ocean. Proc. Natl. Acad. Sci. USA **112**: E5972–E5979. doi:10.1073/pnas.1518165112

Amaral-Zettler, L. A., E. A. McCliment, H. W. Ducklow, and S. M. Huse. 2009. A method for studying protistan diversity using massively parallel sequencing of V9 hypervariable regions of small-subunit ribosomal RNA genes. PLoS One **4**: e6372. doi:10.1371/journal.pone.0006372

Ascani, F., and others. 2013. Physical and biological controls of nitrate concentrations in the upper subtropical North Pacific Ocean. Deep-Sea Res. II **93**: 119–134. doi:10.1016/j.dsr2.2013.01.034

Barone, B., A. R. Coenen, S. J. Beckett, D. J. McGillicuddy Jr., J. S. Weitz, and D. M. Karl. 2019. The ecological and biogeochemical state of the North Pacific subtropical gyre is linked to sea surface height. J. Mar. Res. **77**: 215–245. doi:10.1357/002224019828474241

Benitez-Nelson, C. R., and others. 2007. Mesoscale eddies drive increased silica export in the subtropical Pacific Ocean. Science **316**: 1017–1021. doi:10.1126/science.1136221

Bidigare, R. R., and others. 2009. Subtropical ocean ecosystem structure changes forced by North Pacific climate variations. J. Plankton Res. **31**: 1131–1139. doi:10.1093/plankt/fbp064

Bidigare, R. R., L. Van Heukelem, and C. C. Trees. 2005. Analysis of algal pigments by high-performance liquid chromatography, p. 327–345. *In* R. A. Andersen [ed.], Algal culturing techniques. Academic Press.

Bidigare, R. R., F. R. Buttler, S. J. Christensen, B. Barone, D. M. Karl, and S. T. Wilson. 2014. Evaluation of the utility of xanthophyll cycle pigment dynamics for assessing upper ocean mixing processes at Station ALOHA. J. Plankton Res. **36**: 1423–1433. doi:10.1093/plankt/fbu069

Brainerd, K. E., and M. C. Gregg. 1995. Surface mixed and mixing layer depths. Deep-Sea Res. I **42**: 1521–1543. doi:10.1016/0967-0637(95)00068-H

Bryant, J. A., F. O. Aylward, J. M. Eppley, D. M. Karl, M. J. Church, and E. F. DeLong. 2016. Wind and sunlight shape microbial diversity in surface waters of the North Pacific subtropical gyre. ISME J. **10**: 1308–1322. doi:10.1038/ismej. 2015.221

Calil, P. H. R., and K. J. Richards. 2010. Transient upwelling hot spots in the oligotrophic North Pacific. J. Geophys. Res. Ocean. **115**: C02003. doi:10.1029/2009JC005360

Campbell, L., and D. Vaulot. 1993. Photosynthetic picoplankton community structure in the subtropical North Pacific Ocean near Hawaii (Station ALOHA). Deep-Sea Res. I **40**: 2043–2060. doi:10.1016/0967-0637(93)90044-4

Caporaso, J. G., and others. 2010. QIIME allows analysis of high-throughput community sequencing data. Nat. Methods **7**: 335–336. doi:10.1038/nmeth.f.303

Caron, D. A., and others. 2017. Probing the evolution, ecology and physiology of marine protists using transcriptomics. Nat. Rev. Microbiol. **15**: 6–20. doi:10.1038/nrmicro. 2016.160

Carpenter, S., B. Walker, J. M. Anderies, and N. Abel. 2001. From metaphor to measurement: Resilience of what to what? Ecosystems **4**: 765–781. doi:10.1007/s10021-001-0045-9

Chelton, D. B., M. G. Schlax, R. M. Samelson, and R. A. DeSzoeke. 2007. Global observations of large oceanic eddies. Geophys. Res. Lett. **34**: L15606. doi:10.1029/2007GL030812

Chelton, D. B., P. Gaube, M. G. Schlax, J. J. Early, and R. M. Samelson. 2011. The influence of nonlinear mesoscale eddies on near-surface oceanic chlorophyll. Science **334**: 328–332. doi:10.1126/science.1208897

Choi, C. J., and others. 2020. Seasonal and geographical transitions in eukaryotic phytoplankton community structure in the Atlantic and Pacific Oceans. Front. Microbiol. **11**: 542372. doi:10.3389/fmicb.2020.542372

Church, M. J., C. Mahaffey, R. M. Letelier, R. Lukas, J. P. Zehr, and D. M. Karl. 2009. Physical forcing of nitrogen fixation and diazotroph community structure in the North Pacific subtropical gyre. Global Biogeochem. Cycles **23**: GB2020. doi:10.1029/2008GB003418

Corno, G., D. M. Karl, M. J. Church, R. M. Letelier, R. Lukas, R. R. Bidigare, and M. R. Abbott. 2007. Impact of climate forcing on ecosystem processes in the North Pacific subtropical gyre. J. Geophys. Res. **112**: C04021. doi:10.1029/2006JC003730

Cullen, J. J., P. J. S. Franks, D. M. Karl, and A. Longhurst. 2002. Physical influences on marine ecosystem dynamics, p. 297–336. *In* A. R. Robinson, J. J. McCarthy, and B. J. Rothschild [eds.], The Sea. **12**. John Wiley & Sons, Inc.

DeLong, E. F., and others. 2006. Community genomics among stratified microbial assemblages in the ocean's interior. Science **311**: 496–503. doi:10.1126/science.1120250

Dimier, C., C. Brunet, R. Geider, and J. Raven. 2009. Growth and photoregulation dynamics of the picoeukaryote *Pelagomonas calceolate* in fluctuating light. Limnol. Oceanogr. **54**: 823–836. doi:10.4319/lo.2009.54.3.0823

DiTullio, G. R., and E. A. Laws. 1991. Impact of an atmospheric-oceanic disturbance on phytoplankton community dynamics in the North Pacific central gyre. Deep-Sea Res. A **38**: 1305–1329. doi:10.1016/0198-0149(91)90029-F

Dore, J. E., and D. M. Karl. 1996. Nitrite distributions and dynamics at Station ALOHA. Deep-Sea Res. II **43**: 385–402. doi:10.1016/0967-0645(95)00105-0

Dufois, F., N. J. Hardman-Mountford, J. Greenwood, A. J. Richardson, M. Feng, and R. J. Matear. 2016. Anticyclonic eddies are more productive than cyclonic eddies in subtropical gyres because of winter mixing. Sci. Adv. **2**: e1600282. doi:10.1126/sciadv.1600282

Folke, C., S. Carpenter, B. Walker, M. Scheffer, T. Elmqvist, L. Gunderson, and C. S. Holling. 2004. Regime shifts, resilience, and biodiversity in ecosystem management. Annu. Rev. Ecol. Evol. Syst. **35**: 557–581. doi:10.1146/annurev. ecolsys.35.021103.105711

Garside, C. 1982. A chemiluminescent technique for the determination of nanomolar concentrations of nitrate and nitrite in seawater. Mar. Chem. **11**: 159–167. doi:10.1016/0304-4203(82)90039-1

Giovannoni, S. J., and K. L. Vergin. 2012. Seasonality in ocean microbial communities. Science **335**: 671–676. doi:10.1126/science.1198078

Guillou, L., and others. 2013. The Protist ribosomal reference database (PR2): A catalog of unicellular eukaryote small sub-unit rRNA sequences with curated taxonomy. Nucleic Acids Res. **41**: D597–D604. doi:10.1093/nar/gks1160

Hartmann, M., C. Grob, G. A. Tarran, A. P. Martin, P. H. Burkill, D. J. Scanlan, and M. V. Zubkov. 2012. Mixotrophic basis of Atlantic oligotrophic ecosystems. Proc. Natl. Acad. Sci. USA **109**: 5756–5760. doi:10.1073/pnas.1118179109

Hayward, T. L., and J. L. McGowan. 1979. Pattern and structure in an oceanic zooplankton community. Am. Zool. **19**: 1045–1055. doi:10.1093/icb/19.4.1045

Holling, C. S. 1973. Resilience and stability of ecological systems. Annu. Rev. Ecol. Evol. Syst. **4**: 1–23.

Hu, S. K., P. E. Connell, L. Y. Mesrop, and D. A. Caron. 2018. A hard day's night: Diel shifts in microbial eukaryotic activity in the North Pacific subtropical gyre. Front. Mar. Sci. **5**: 351. doi:10.3389/fmars.2018.00351

Huisman, J., N. N. Pham Thi, D. M. Karl, and B. Sommeijer. 2006. Reduced mixing generates oscillations and chaos in the oceanic deep chlorophyll maximum. Nature **439**: 322–325. doi:10.1038/nature04245

Ives, A. R., and S. R. Carpenter. 2007. Stability and diversity of ecosystems. Science **317**: 58–62. doi:10.1126/science.1133258

Johnson, K. S., S. C. Riser, and D. M. Karl. 2010. Nitrate supply from deep to near-surface waters of the North Pacific subtropical gyre. Nature **465**: 1062–1065. doi:10.1038/nature09170

Karl, D. M. 1999. A sea of change: Biogeochemical variability in the North Pacific subtropical gyre. Ecosystems **2**: 181–214. doi:10.1007/s100219900068

Karl, D. M. 2002. Nutrient dynamics in the deep blue sea. Trends Microbiol. **10**: 410–418. doi:10.1016/S0966-842X(02)02430-7

Karl, D. M., and M. J. Church. 2014. Microbial oceanography and the Hawaii Ocean Time-series programme. Nat. Rev. Microbiol. **12**: 699–713. doi:10.1038/nrmicro3333

Karl, D. M., and M. J. Church. 2017. Ecosystem structure and dynamics in the North Pacific subtropical gyre: New views of an old ocean. Ecosystems **20**: 433–457. doi:10.1007/s10021-017-0117-0

Karl, D. M., and R. Lukas. 1996. The Hawaii Ocean Time-series (HOT) program: Background, rationale and field implementation. Deep-Sea Res. II **43**: 129–156. doi:10.1016/0967-0645(96)00005-7

Karl, D. M., and G. Tien. 1992. MAGIC: A sensitive and precise method for measuring dissolved phosphorus in aquatic environments. Limnol. Oceanogr. **37**: 105–116. doi:10.4319/lo.1992.37.1.0105

Karl, D. M., R. M. Letelier, D. Hebel, L. Tupas, J. Dore, J. Christian, and C. Winn. 1995. Ecosystem changes in the North Pacific subtropical gyre attributed to the 1991-92 El Niño. Nature **373**: 230–234. doi:10.1038/373230a0

Karl, D. M., R. R. Bidigare, and R. M. Letelier. 2003. Sustained and aperiodic variability in organic matter production and phototrophic microbial community structure in the North Pacific subtropical gyre, p. 222–264. *In* P. J. le, B. Williams, D. N. Thomas, and C. S. Reynolds [eds.], Phytoplankton productivity: Carbon assimilation in marine and freshwater ecosystems. Blackwell Science.

Karl, D. M., R. M. Letelier, R. R. Bidigare, K. M. Björkman, M. J. Church, J. E. Dore, and A. E. White. 2021. Seasonal-to-decadal scale variability in primary production and particulate matter export at Station ALOHA. Prog. Oceanogr. **195**: 102563. doi:10.1016/j.pocean.2021.102563

Keeling, P. J., and F. Burki. 2019. Progress towards the tree of eukaryotes. Curr. Biol. **29**: R808–R817. doi:10.1016/j.cub.2019.07.031

Letelier, R. M., R. R. Bidigare, D. V. Hebel, M. Ondrusek, C. D. Winn, and D. M. Karl. 1993. Temporal variability of phytoplankton community structure based on pigment analysis. Limnol. Oceanogr. **38**: 1420–1437. doi:10.4319/lo.1993.38.7.1420

Letelier, R. M., D. M. Karl, M. R. Abbott, P. Flament, M. Freilich, R. Lukas, and T. Strub. 2000. Role of late winter mesoscale events in the biogeochemical variability of the upper water column of the North Pacific subtropical gyre. J. Geophys. Res. **105**: 28723–28739. doi:10.1029/1999JC000306

Lévy, M., P. J. S. Franks, and K. S. Smith. 2018. The role of submesoscale currents in structuring marine ecosystems. Nat. Commun. **9**: 4758. doi:10.1038/s41467-018-07059-3

Li, B., D. Karl, R. Letelier, R. Bidigare, and M. J. Church. 2013. Temporal and depth variability of chromophytic phytoplankton in the North Pacific subtropical gyre. Deep-Sea Res. II **93**: 84–95. doi:10.1016/j.dsr2.2013.03.007

Mahaffey, C., K. M. Björkman, and D. M. Karl. 2012. Phytoplankton response to deep seawater nutrient addition in the North Pacific subtropical gyre. Mar. Ecol. Prog. Ser. **460**: 13–34. doi:10.3354/meps09699

Margalef, R. 1978. Life-forms of phytoplankton as survival alternatives in an unstable environment. Oceanol. Acta **1**: 493–509.

McGillicuddy, D. J., and others. 1998. Influence of mesoscale eddies on new production in the Sargasso Sea. Nature **394**: 263–266. doi:10.1038/28367

McMurdie, P. J., and S. Holmes. 2013. Phyloseq: An R package for reproducible interactive analysis and graphics of microbiome census data. PLoS One **8**: e61217. doi:10.1371/journal.pone.0061217

Mende, D. R., J. A. Bryant, F. O. Aylward, J. M. Eppley, T. Nielsen, D. M. Karl, and E. F. DeLong. 2017. Environmental drivers of a microbial genomic transition zone in the ocean's interior. Nat. Microbiol. **2**: 1367–1373. doi:10.1038/s41564-017-0008-3

Oksanen, J., and others. 2013. Package 'vegan': Community ecology package. R package version 2.0-10. http://cran.r-project.org/web/packages/vegan/.

Ollison, G. A., S. K. Hu, L. Y. Mesrop, E. F. DeLong, and D. A. Caron. 2021. Come rain or shine: Depth not season shapes the active protistan community at Station ALOHA in the North Pacific subtropical gyre. Deep-Sea Res. I **170**: 103494. doi:https://doi.org/10.1016/j.dsr.2021.103494

Pickett, S., J. Kolasa, J. Armesto, and S. Collins. 1989. The ecological concept of disturbance and its expression at various hierarchical levels. Oikos **54**: 129–136. doi:10.2307/3565258

Polovina, J. J., E. A. Howell, and M. Abecassis. 2008. Ocean's least productive waters are expanding. Geophys. Res. Lett. **35**: L03618. doi:10.1029/2007GL031745

Quast, C., and others. 2013. The SILVA ribosomal RNA gene database project: Improved data processing and web-based tools. Nucl. Acids Res. **41**: D590–D596. doi:10.1093/nar/gks1219

Reynolds, C. S., J. Padisák, and U. Sommer. 1993. Intermediate disturbance in the ecology of phytoplankton and the maintenance of species diversity: A synthesis. Hydrobiologia **249**: 183–188. doi:10.1007/BF00008853

Rii, Y. M., D. M. Karl, and M. J. Church. 2016. Temporal and vertical variability in picophytoplankton primary productivity in the North Pacific subtropical gyre. Mar. Ecol. Prog. Ser. **562**: 1–18. doi:10.3354/meps11954

Rii, Y. M., R. R. Bidigare, and M. J. Church. 2018. Differential responses of eukaryotic phytoplankton to nitrogenous nutrients in the North Pacific subtropical gyre. Front. Mar. Sci. **5**: 92. doi:10.3389/fmars.2018.00092

Rykiel, E. J., Jr. 1985. Towards a definition of ecological disturbance. Austral Ecol. **10**: 361–365. doi:10.1111/j.1442-9993.1985.tb00897.x

Sarmiento, J. L., T. M. C. Hughes, R. J. Stouffer, and S. Manabe. 1998. Simulated response of the ocean carbon cycle to anthropogenic climate warming. Nature **393**: 245–249. doi:10.1038/30455

Shade, A., and others. 2012. Fundamentals of microbial community resistance and resilience. Front. Microbiol. **3**: 417. doi:10.3389/fmicb.2012.00417

Stommel, H. 1963. Varieties of oceanographic experience. Science **139**: 572–576. doi:10.1126/science.139.3555.572

Sugihara, G., and R. M. May. 1990. Nonlinear forecasting as a way of distinguishing chaos from measurement error in time series. Nature **344**: 734–741. doi:10.1038/344734a0

Sverdrup, H. U. 1953. On conditions for the vernal blooming of phytoplankton. J. Cons. Explor. Mer. **18**: 287–295.

de Vargas, C., and others. 2015. Eukaryotic plankton diversity in the sunlit ocean. Science **348**: 1261605. doi:10.1126/science.1261605

Venrick, E. L. 1993. Phytoplankton seasonality in the central North Pacific: The endless summer reconsidered. Limnol. Oceanogr. **38**: 1135–1149. doi:10.4319/lo.1993.38.6.1135

Venrick, E. L. 1997. Comparison of the phytoplankton species composition and structure in the Climax area (1973-1985) with that of Station ALOHA (1994). Limnol. Oceanogr. **42**: 1643–1648. doi:10.4319/lo.1997.42.7.1643

Venrick, E. L. 1999. Phytoplankton species structure in the central North Pacific, 1973-1996: Variability and persistence. J. Plankton Res. **21**: 1029–1042. doi:10.1093/plankt/21.6.1029

Walker, B., C. S. Holling, S. R. Carpenter, and A. Kinzig. 2004. Resilience, adaptability and transformability in social-ecological systems. Ecol. Soc. **9**: 5. doi:10.5751/ES-00650-090205

Wickham, H. 2009. ggplot2: Elegant graphics for data analysis, 2nd ed. Springer.

Wilson, S. T., B. Barone, F. Ascani, and others. 2015. Short-term variability in euphotic zone biogeochemistry and primary productivity at Station ALOHA: A case study of summer 2012. Global Biogeochem. Cycles **29**: 1145–1164. doi:10.1002/2015GB005141

Worden, A., J. Nolan, and B. Palenik. 2004. Assessing the dynamics and ecology of marine picophytoplankton: The importance of the eukaryotic component. Limnol. Oceanogr. **49**: 168–179. doi:10.4319/lo.2004.49.1.0168

Conflict of Interest

None declared.